

***Interactive comment on “Uncertainty analysis of a European high-resolution emission inventory of CO<sub>2</sub> and CO to support inverse modelling and network design” by Ingrid Super et al.***

We would like to thank the reviewers for their enthusiasm about our study and for the comments on our work. The review comments have been helpful in reflecting on our work and pointing out parts that required further improvements. Below we address specific issues mentioned by the reviewers point by point. The manuscript has been updated accordingly (changes are highlighted, line numbers refer to the final manuscript).

***Anonymous Referee #1 Received and published: 18 October 2019***

*Review of "Uncertainty analysis of a European high-resolution emission inventory of CO<sub>2</sub> and CO to support inverse modelling and network design" by Super et al.*

*This manuscript describes an effort to construct an anthropogenic CO<sub>2</sub> and CO inventory for a portion of Europe with carefully constructed uncertainties. The authors also show some basic analysis of their results, comparing uncertainties in different sectors and between countries, and the effect of some uncertainties on concentrations on CO<sub>2</sub> or CO in the atmosphere. It is well-written, relevant, and extremely thorough, and should be published in ACP. The only major comment I have is about the data availability statement. The data availability requirement for publication has not been met: data is only available by request to authors, which is not acceptable to this journal, I believe. Even if it is, I think the data (i.e. the inventory and uncertainties) should be made available publicly and without restriction, especially as I think this product would be of interest to many researchers.*

We thank the reviewer for this suggestion. We agree that the data is useful for many researchers and have made the data accessible through Zenodo (see Data Availability description).

*Otherwise, my comments are fairly minor, and detailed below.*

*Introduction: Please define TNO the first time to define the acronym for international readers.*

We have replaced TNO by ‘the Netherlands Organisation for Applied Scientific Research (TNO)’ in lines 35-36.

*L33 - How are the national numbers determined for reporting? These are also inventories, presumably of the scaled-up variety? perhaps the authors can make this section more specific to inventories that are spatially gridded and temporally downscaled, perhaps those commonly used for atmospheric studies?*

The reported country-level emissions are available from UNFCCC (<https://unfccc.int/process-and-meetings/transparency-and-reporting/reporting-and-review-under-the-convention/greenhouse-gas-inventories-annex-i-parties/national-inventory-submissions-2019>) and based on energy statistics and emission factors following IPCC guidelines and are calculated as national, yearly total. This has been clarified in lines 32-34. In some cases IPCC default values are used, but countries can also decide to use country-specific values (which are generally more realistic). There is no scaling involved here, except that the overall energy consumption for one sector is divided over several sub-sectors. This introduces some uncertainty, which is taken into account in the uncertainty definition for the activity data listed in Appendix A.

*L51: I am left wondering what a Tier 3 consists of in this regard, which the US EPA follows I believe.*

It should be noted that there are two types of calculations with respect to emission reporting: calculation of the emissions and calculation of the emission uncertainties. The IPCC describes only the Tier 1 and Tier 2 approach for calculating emission uncertainties. In contrast, there is also a Tier 3 approach for calculation of emissions, which uses country-specific data and models. The Tier 3 approach used by the US EPA is therefore related to calculation of the emissions, and not of the emission uncertainties. In short, there are 3 Tiers for emission calculation and 2 Tiers for uncertainties.

*L72: What is H2020?*

H2020 is short for Horizon 2020, a European Research and Innovation programme. This is clarified in lines 77-78.

*L72: Should be made public, not on request - Journal editors can decide on this but that is my understanding of current publishing policy.*

We agree and have made the data accessible through Zenodo (see Data Availability description).

*L70-76: These sentences are not actually very clear as to what the work is and confuse the reader. Are the 10 inventories part of this work, or only the new high-resolution inventory for the zoom region? No doubt this will be made clear later in the paper but should be outlined here.*

We have clarified that the methodology used to create the family of emission inventories is also used in the work described in this manuscript (lines 78-79).

*L81: Should read: ... (12-16h LT) emissions, which could be the only emissions optimized in a study with a small domain, such as a city, using only afternoon observations? [if a study is regional or the city is large, then using mid-afternoon observations will still allow optimization of early morning emissions for example, depending on wind speed and location of emissions relative to the measurement point, for example]. But I absolutely agree that looking at the temporal variability and whether that is correct can be crucial in an urban study as well as a regional one (as illustrated by Hu et al. Science Advances 2019 for continental work). It may be an issue even if the inversion is sensitive to all hours.*

For clarity this topic has been introduced earlier in the introduction (lines 66-70), so that more explanation can be given.

*L108. Comma should be a period.*

Done.

*L108: if it's not described later, an additional sentence on the temporal disaggregation would be nice (does it account for weekday/weekend effects for example?).*

The time profiles are described in more detail in Section 2.2.4 (lines 207-213). Although a weekly cycle is included, e.g. with lower traffic emissions during the weekend, the diurnal profile is the same for weekdays and weekends.

*L109: What is GNFR vs. NFR?*

NFR sectors are very detailed and aggregated to GNFR sectors, i.e. GNFR is the aggregated version of NFR used for delivering gridded inventory data (the “G” stands for Gridding) (line 119). This is now also mentioned in the caption of Table 2.

*L138: is the point source data also temporally explicit? I am specifically thinking of energy generation (e.g. gas or coal-fired power plants, whose hour-to-hour emissions can vary drastically with no predictable cycle, at least in the U.S.).*

The point sources get the same temporal distribution as the area sources, using the fixed time profiles. This has been made more clear in lines 148-149. We have previously studied daily activity from some major power plants and found that, indeed, the temporal variations in emissions from power plants is difficult to describe with environmental variables. Unfortunately, temporally detailed activity data is not broadly available and therefore not part of the emission inventory. This is an important point for the future, which is now also mentioned in lines 594-595.

*Fig. 2: I understand from the text that correlations between sub-sectors are accounted for, but as this (and the next) figure shows aggregated sectors and no off-diagonal terms (i.e. no correlations in the uncertainties between sectors), why show these in this manner? Is the color axis in units of emissions, or do they range from 0-1 because they are covariances? (I would think the former, or they would all be 1 on the diagonal?). Or am I missing something here. Please clarify.*

Error correlations exist between several sub-sectors that are part of the same aggregated (GNFR) sector. Therefore, no off-diagonal values are visible, i.e. there are no error correlations between GNFR sectors. The reason that the uncertainties are displayed in this manner (covariance matrix) is because this is the common way to describe prior uncertainties for inversion studies. They are indeed covariances, ranging from 0 to 1.

*L218: should read "it is important to ensure"...*

Done.

*L234 define MC as Monte Carlo earlier*

The abbreviation MC has been replaced with the full name ‘Monte Carlo’ throughout the manuscript.

*Fig 7 & 8: Captions should indicate left and right panels, for example "Contribution of source sectors to the total uncertainty in CO<sub>2</sub> (left) and CO (right) emissions, summing to 100 %."*

*Same for Fig 9, it is easy enough to just say (left) and (right) in the caption here.*

These indications have been added consistently to all figure captions.

*To clarify for fig 10&11, these spreads in concentration are from the experiments using different random emissions maps, i.e. the model was run 500 times, correct?*

Yes, this is correct. This is now mentioned in line 293-294 and the figure captions.

*Fig 11 - I find this to be a very interesting analysis. It points to whether we expect an inversion to identify the true location of these 20 plants among all these scenarios. I.e. can some of the maps be shown to be false by the observed CO<sub>2</sub>? The large spread indicates maybe so, but then again, once all the other sources and their uncertainty are included, it would likely be pretty hard!*

Yes, we agree that it will be very challenging. Also given the uncertainty introduced by the model transport, which would likely be similar or larger than (depending on the complexity of the area) the spread caused by the different maps. Nevertheless, we show here that it is an important source of uncertainty for local inversions.

*Section 3.3: inversion usually does not only include time from 12-16, just because those are the observation times. You may be optimizing emissions from earlier in the day, depending on the domain size and wind speeds. This should just be noted.*

We have added a sentence that explains that our reasoning only applies to local studies (lines 420-421).

*Fig 12 and text related: this standard time profile (black) seems to have a monthly mean that is then also distributed hourly through the day? Is it hourly, or 3-hourly? weekday/weekend (for businesses vs. residences, assuming those are contributing to stationary combustion for on-site heating, e.g. burning of gas)? These details could be mentioned in the caption, I realize they are not necessary for describing the uncertainty method, but they are useful to know for users of the inventory emissions.*

For each sector there are three temporal profiles: a profile describing the seasonal cycle (monthly factors), a profile describing day-to-day variations (daily factors) and a profile describing the diurnal cycle (hourly factors). This is now described in more detail in lines 207-213.

*Fig 14, the text on the map, especially "Tirol" and "Hotspot", is hard to see here perhaps larger, or placed in a different section with an arrow to the appropriate box?*

Both Fig. 14 and Fig. 15 have been improved by increasing the weight of the boxes and the font size.

*L475: Does this statement refer to their methods for calculating emissions or uncertainties?*

Actually both, but in this case we mean the uncertainty calculation. This is clarified in line 503.

*Data Availability: See note at top, this data should be publicly available on a public-facing data portal.*

Data are now publicly available. The Data Availability section has been updated accordingly.

***Anonymous Referee #2 Received and published: 21 October 2019***

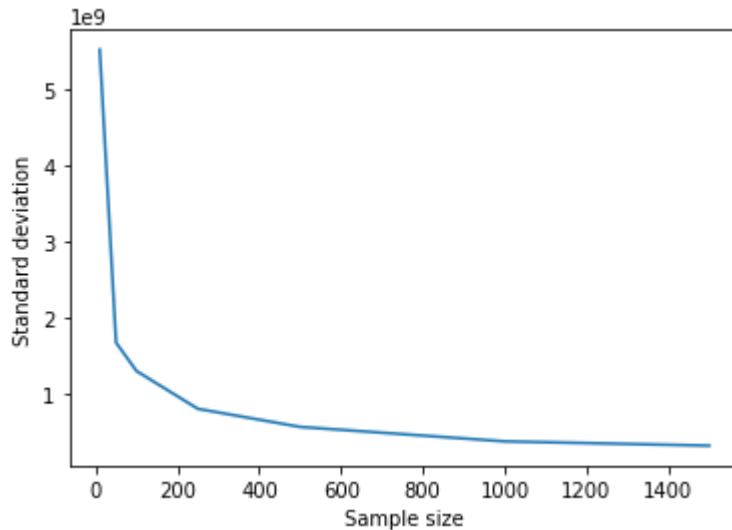
*This manuscript presents an assessment of the uncertainties in high-resolution emission inventories of CO<sub>2</sub> and CO in 14 European countries. The uncertainties present in various underlying parameters of the inventories (e.g., absolute uncertainties in reported emissions, emission factors, spatial proxies, temporal profiles) are propagated using a well-described Monte Carlo simulation routine. The uncertainties are tracked to assess the importance of specific source sectors in introducing large uncertainties on both absolute and relative bases. Several factors are found to be playing an important role in contributing to the final emission uncertainties. For instance, spatial disaggregation of the emissions at a high spatial resolution results in large uncertainties at the local/city scale, which has important implications for inverse modeling studies operating within these smaller spatial domains. The authors find that because certain sectors with large overall contribution of CO<sub>2</sub> and CO emissions are well-constrained (e.g., industrial sector in the Paris metro area), the relative uncertainties in these locations are far smaller than those in the immediate rural surroundings. Thus, future efforts to reduce absolute emissions of CO<sub>2</sub> and CO may use the absolute uncertainties presented in this study to identify a network of key target areas/sectors.*

*Overall, I find this manuscript well-written. The methods are presented in sufficient detail that one could reproduce them. The methods section lacks some quality assurance, as I have described in my first major comment. The results are presented in an organized fashion, and the interpretations and conclusions are generally well-reasoned. My second major comment has to do with the framing of these interpretations with respect to observation-based literature, especially since the authors mention a motivation for this study is to facilitate inter-comparison of modeled and observed greenhouse gas concentrations. Once the authors have addressed these comments adequately, the manuscript should be ready for publication in ACP. In addition to my two major comments, I list several minor comments that are mostly typographical errors and/or suggestions to improve presentation of figures and tables.*

*Major comments:*

*1. A rationale for number of Monte Carlo (MC) simulations should be provided. For e.g., a plot with some metric of quality of results (total residual, total error, fullwidth half maximums of the distributions showed in Fig. 7, etc.) versus number of MC runs. I'd expect such a plot to have an exponential decay with respect to increasing MC runs, which would then help justify the choice of  $N = 500$ .*

Because the Monte Carlo simulations performed in this study are relatively cheap the sample size can be taken large enough to ensure a robust result. However, to support our choice for  $N=500$  we used two methods described in literature: sampling statistics and bootstrapping. Both methods give similar curves, such as shown below. The curve indicates the spread in the standard deviations if we would repeat the Monte Carlo simulation multiple times for a specific sample size, i.e. it indicates how robust the uncertainty estimate is. From this figure we conclude that a sample size larger than 500 would not increase the robustness a lot.



We have added a statement that a sample size of  $N=500$  is large enough to get robust results, based on the analysis shown here (lines 249-250). For completeness, we have added this figure to Appendix B.

Reference:

Janssen, H.: Monte-Carlo based uncertainty analysis: Sampling efficiency and sampling convergence. *Reliability Engineering & System Safety*, 109, 123-132, <https://doi.org/10.1016/j.ress.2012.08.003>, 2013.

2. *I think the presentation of the results could be better framed with respect to other literature. For instance, the authors show that the spread in their modeled CO<sub>2</sub> and CO concentrations reduces over distances of 5–40 km from the source categories (Figures 10 and 11). How does this length-scale compare with other studies? Are there any monitoring studies that have shown similar fall-off length-scales? To say that road transport affects CO concentration as far as 40 km downwind seems excessive, if one were to compare it to, say, Figure 4A from Canagaratna et al.'s mobile monitoring study.*

We agree with the reviewer that we have not discussed this topic in our paper. Instead, we have focused our discussion on the estimated uncertainties in the (gridded) emissions, which is the main topic of our paper and covers most of our results. However, we have put some effort in improving the comparison of the model results with other literature, mainly to explain how these model results can be used for network design and inverse modelling (lines 499-501 and lines 570-585).

*Minor comments:*

1. L24: *I suggest using “abundant”, instead of “important”. In terms of warming potential, there are other gases more important than CO<sub>2</sub> (e.g., CH<sub>4</sub>).*

We have replaced this word.

2. L36: *“report”, not “reported”.*

The sentence has been rephrased for clarification (line 37).

3. L69: *“atmospheric”, not “atmospherics”.*

Done.

4. L64-65: *“in contrast, if... are needed.” This sentence is unclear. What is “prior” referring to? Please reword.*

In inverse modelling the word ‘prior’ refers to the initial emission inventory, containing information on the order of magnitude and location of emissions which is then updated using atmospheric observations. This has been clarified in line 65.

5. L76-77: *not sure what “European zoom region” means. Please clarify.*

We have clarified which region is meant in line 84.

6. L81: *suggest replacing “time profiles” with “temporal profiles”, or “diurnal profiles”.*

We have replaced ‘time profiles’ with ‘temporal profiles’ throughout the manuscript.

7. L81-83: *question 3 is somewhat unclear. It could be reworded for clarity, but also the motivation for this question was not set up in the introduction. This makes this question feel abruptly added.*

This topic has now been introduced in lines 66-70 for clarification.

8. L86: *is “partitioning” the right word? I suggest using “apportionment”, instead.*

This word has been replaced in line 94.

9. Table 1: *for consistency with first usage in L26, please continue with the “FFCO”, “FFCO2” naming conventions. The acronyms FF and BF should be declared in the Table caption. Also, is there a specific reason to use three-letter country codes, instead of simply country names?*

The names of the species have been updated and FF and BF are explained in the caption of Table 1. Also, the names of the countries have been given.

10. L103: *“gap-filled” (should be hyphenated).*

Done.

11. L103: *suggest replacing “data was gap filled” with something more informative of which attributes of the dataset were missing, and how they were filled (i.e., with NaNs, or geospatial interpolated, etc.).*

The gap-filling refers to the reported emissions, which are sometimes missing for specific sectors. Also, in some cases the reported data is considered to be unreliable. In those cases, other sources of information are used to update and complete the emission inventory. This is now explained in more detail in lines 112-113.

12. L105: acronym “AIS” not defined.

The acronym has been defined in line 115.

13. L108: comma is used instead of period.

The comma has been replaced.

14. L109: acronym “GNFR” not defined, and is also used in Table 2 without definition.

GNFR is the aggregated version of NFR. This is now mentioned in the caption of Table 2.

15. Figure 1: could the authors add a few landmarks or identify a few of the visible hotspots in these maps e.g., Paris? It’d be helpful for a reader not familiar with the placement of major urban areas of Europe.

Figure 1 has been updated and indicates the location of some major urban areas (Paris, Ruhr area and Rotterdam).

16. L148: which “differences” are being referred to in this sentence? Differences in uncertainties, I assume? Should be clarified.

Indeed, this has been made explicit in line 159-160.

17. Figures 2 and 3: the gridlines need to match the category labels. The current version of this figure is difficult to read easily.

We choose to match the gridlines with the category labels, such that the intersection of two lines clearly indicates the value belonging to those categories. But if we understand correctly the reviewer would like to see the gridlines surrounding each entry in the matrix, instead of being in the middle of each row/column. This has been updated.

18. L294-296: This sentence is confusing. Here is how I would calculate the “uncertainty in the total emissions”: a) take the standard deviations of emissions from each sector (i.e., standard deviation of each box in Figure 7-left), b) calculate the average of the standard deviations from (a), and c) report this average from (b) as “uncertainty in total emissions”. However, it seems the authors have used a different approach: a) take the standard deviations of emissions from each sector (i.e., standard deviation of each box in Figure 7-left), b) calculate the STANDARD DEVIATION of the standard deviations from (a), and c) report this STANDARD DEVIATION from (b) as “uncertainty in total emissions”. Is this correct? If yes, this would not be the “uncertainty in total emissions”, but rather would be an “uncertainty of the uncertainty in total emissions”. Please justify/clarify/correct in the manuscript accordingly.

The uncertainty in the total emissions is calculated from the Monte Carlo, similarly as the uncertainty for each sector. The Monte Carlo provides 500 solutions for each of the defined sub-sectors (NFR – fuel combination). These are summed to get 500 solutions for GNFR sector emissions. If we then sum the GNFR sector emissions we get 500 solutions for the total emission. What is reported here is the standard deviation of these 500 solutions. We have clarified this in lines 309-311.



19. Figures 8, 9, and 16: As I indicated in my initial review prior to posting on ACPD, the legend needs to be reversed to be consistent with the order of stacking.

The order of the legends has been reversed.

20. L322-323: “Overall, the differences between countries are relatively small(Figure 9, right panel).” Instead of using a qualitative term like “relatively small”, why not report the total uncertainty as done for Figure 7?

We have presented the range of standard deviations, which is between 1.2 and 2.3% (lines 339-341).

21. L339: “For CO<sub>2</sub> (left panel) we see a concentration of about ...” should be changed to “For CO<sub>2</sub> (left panel), we see a spread in concentration of about ...” There is no information in Figure 10 about the absolute CO<sub>2</sub> concentrations, so seeing a concentration of 3 ppm anywhere in ambient air would be impossible. A related suggestion is to plot the absolute numbers on the right axis, to get a better sense of the absolute concentrations (especially for CO).

We agree that these concentrations are not what you would measure in the atmosphere. Rather, they are the result only of the emissions of stationary combustion (CO<sub>2</sub>) and road transport (CO). This has been clarified in the text (lines 357-358).

22. L343: what does “atmospheric signal” mean? Why not just say “modeled spread in concentration”?

What we refer to is the concentration enhancement caused by the specified sector. We have replaced ‘signal’ by ‘concentration enhancement’ throughout the text.

23. Figures 10 and 11: the x-axis labels are unevenly spaced. It is definitely not linear, but it doesn’t seem log-spaced either. Please correct/clarify in Figure caption.

The labels are unevenly spaced, because we only added labels for the distances that we have included in the model simulations. Nevertheless, the axis is linear.

24. Figure 12: Please describe what the grey lines represent in the caption.

The grey lines represent the spread in the temporal profile, resulting from the Monte Carlo simulation. This is clarified in the caption.

25. L397: “in inverse modeling, often ... transport”. It’d be good to include a couple of references to support this statement.

See lines 419-420 for the references.

26. Figure 13: I know that time profiles used for modeling CO<sub>2</sub> and CO emissions are the same, but it’d be good to rename the y-axis label to “normalized spread in CO<sub>2</sub> and CO emissions”, and remind the reader of this very briefly in the caption.

We have added this comment to the figure caption.

27. L447: “big cities like Paris, Berlin, and Brussels”. I assume this is about the CO, and not the CO2 map? It’d help to point to these cities in Figure 15.

Indeed, this part describes relative uncertainties in CO (as is also mentioned in the caption of Figure 17). We have added this to line 472. For clarity, we have replaced the current list with those urbanized areas now shown in Fig. 1, including a reference to this figure (line 471-472).

28. L528: no need to define the acronym LTO, if it is only used once.

The term LTO has been removed.

*Reference(s): Canagaratna, M. R.; Onasch, T. B.; Wood, E. C.; Herndon, S. C.; Jayne, J. T.; Cross, E. S.; Miake-Lye, R. C.; Kolb, C. E.; Worsnop, D. R. Evolution of vehicle exhaust particles in the atmosphere. J. Air Waste Manag. Assoc. 2010, 60 (10), 1192–1203.*

1 **Uncertainty analysis of a European high-resolution emission**  
2 **inventory of CO<sub>2</sub> and CO to support inverse modelling and**  
3 **network design**

4 Ingrid Super<sup>1</sup>, Stijn N.C. Dellaert<sup>1</sup>, Antoon J.H. Visschedijk<sup>1</sup>, Hugo A.C. Denier van der Gon<sup>1</sup>

5 <sup>1</sup>Department of Climate, Air and Sustainability, TNO, P.O. Box 80015, 3508 TA Utrecht, Netherlands

6 *Correspondence to:* Ingrid Super ([ingrid.super@tno.nl](mailto:ingrid.super@tno.nl))

7 **Abstract.** Quantification of greenhouse gas emissions is receiving a lot of attention, because of its relevance for  
8 climate mitigation. Complementary to official reported bottom-up emission inventories, Quantification ~~is~~  
9 ~~often~~ can be done with an inverse modelling framework, combining atmospheric transport models, prior gridded  
10 emission inventories and a network of atmospheric observations to optimize the emission inventories. An  
11 important aspect of such method is a correct quantification of the uncertainties in all aspects of the modelling  
12 framework. The uncertainties in gridded emission inventories are, however, not systematically analysed. In this  
13 work, a statistically coherent method is used to quantify the uncertainties in a high-resolution gridded emission  
14 inventory of CO<sub>2</sub> and CO for Europe. We perform a range of Monte Carlo simulations to determine the effect of  
15 uncertainties in different inventory components, including the spatial and temporal distribution, on the uncertainty  
16 in total emissions and the resulting atmospheric mixing ratios. We find that the uncertainty in the total emissions  
17 for the selected domain are 1 % for CO<sub>2</sub> and 6 % for CO. Introducing spatial disaggregation causes a significant  
18 increase in the uncertainty of up to 40 % for CO<sub>2</sub> and 70 % for CO for specific grid cells. Using gridded  
19 uncertainties specific regions can be defined that have the largest uncertainty in emissions and are thus an  
20 interesting target for inverse modelers. However, the largest sectors are usually the best-constrained ones (low  
21 relative uncertainty), so the absolute uncertainty is the best indicator for this. With this knowledge areas can be  
22 identified that are most sensitive to the largest emission uncertainties, which supports network design.

## 23 1 Introduction

24 Carbon dioxide (CO<sub>2</sub>) is the most ~~important-abundant~~ greenhouse gas and is emitted in large quantities from  
25 human activities, especially from the burning of fossil fuels (Berner, 2003). A reliable inventory of fossil fuel CO<sub>2</sub>  
26 (FFCO<sub>2</sub>) emissions is important to increase our understanding of the carbon cycle and how the global climate will  
27 develop in the future. The impact of CO<sub>2</sub> emissions is visible on a global scale and international efforts are required  
28 to mitigate climate change, but cities are the largest contributors to FFCO<sub>2</sub> emissions (about 70% (IEA, 2008)).  
29 Therefore, emissions should be studied at different spatial and temporal scales to get a full understanding of their  
30 variability and mitigation potential.

31 One way of describing emissions is an emission inventory, which is a structured set of emission data,  
32 distinguishing different pollutants and source categories. Often, emission inventories are based on reported  
33 ~~country-level~~ emission data (for example from the National Inventory Reports (NIR's) (UNFCCC, 2019)), ~~which~~  
34 ~~are national, yearly emissions based on energy statistics, which~~ These country-level emissions ~~are~~ can be spatially  
35 and temporally disaggregated (scaled-down) to a certain level using proxies (e.g. the ~~TNO~~ inventories ~~of the~~  
36 ~~Netherlands Organisation for Applied Scientific Research (TNO)~~ (Denier van der Gon et al., 2017; Kuenen et al.,  
37 2014)). Other emission inventories are based on local energy consumption data and reported emissions, ~~which are~~  
38 ~~(dis)~~ aggregated to the required spatial scale (~~scaled-up~~) (e.g. Hestia (Gurney et al., 2011, 2019)) or rely on (global)  
39 statistical data and a consistent set of (non-country specific) emission factors representing different technology  
40 levels (e.g. EDGAR (<http://edgar.jrc.ec.europa.eu>)). Most inventories, including the one used in this study, rely  
41 on a combination of methods, using large-scale data supplemented with local data. Gridded emission inventories  
42 are essential as input for atmospheric transport models to facilitate comparison with observations of CO<sub>2</sub>  
43 concentrations, as well as in inverse modelling as a prior estimate of the emission locations and magnitude.

44 During the compilation of an emission inventory uncertainties are introduced at different levels (e.g. magnitude,  
45 timing or locations) and increasingly more attention is given to this topic. Parties to the United Nations Framework  
46 Convention on Climate Change (UNFCCC) report their annual emissions (disaggregated over source sectors and  
47 fuel types) in a NIR (UNFCCC, 2019), which includes an assessment of the uncertainties in the underlying data  
48 and an analysis of the uncertainties in the total emissions following IPCC (Intergovernmental Panel on Climate  
49 Change) guidelines. The simplest uncertainty analysis is based on simple equations for combining uncertainties  
50 from different sources (Tier 1 approach). A more advanced approach is a Monte Carlo simulation, which allows  
51 for non-normal uncertainty distributions (Tier 2 approach). The Tier 2 approach has been used by several  
52 countries, for example Finland (Monni et al., 2004) and Denmark (Fauser et al., 2011).

53 These reports provide a good first step in quantifying emission uncertainties, but the uncertainty introduced by  
54 using proxies for spatial and temporal disaggregation are not considered. These are, however, an important source  
55 of uncertainty in the gridded emission inventories (Andres et al., 2016). Inverse modelling studies are increasingly  
56 focusing on urban areas, the main source areas of FFCO<sub>2</sub> emissions, for which emission inventories with a high  
57 spatiotemporal resolution are used to better represent the variability in local emissions affecting local  
58 concentration measurements. Understanding the uncertainty at higher resolution than the country-level is thus  
59 necessary, which means that the uncertainty caused by spatiotemporal disaggregation becomes important as well.  
60 The uncertainties in emission inventories are important to understand for several reasons. First, knowledge of  
61 uncertainties helps pinpointing emission sources or areas that require more scrutiny (Monni et al., 2004; Palmer  
62 et al., 2018). Second, knowledge of uncertainties in prior emission estimates is an important part of inverse

63 modelling frameworks, which can be used for emission verification and in support of decision-making (Andres et  
64 al., 2014). For example, if uncertainties are not properly considered, there is a risk that the uncertainty range does  
65 not contain the actual emission value. In contrast, if uncertainties are large overestimated the prior-initial emission  
66 inventory gives little information about the actual emissions and more independent observations are needed. Third,  
67 local inverse modelling studies often rely on daytime (12-16h LT) observations, which are easier to simulate.  
68 Given the small size of the urban domain these observations only contain information on recent emissions, which  
69 have to be extrapolated using temporal profiles to calculate annual emissions. Therefore, knowledge of  
70 uncertainties in temporal profiles helps to better quantify the uncertainty in these annual emissions. Finally,  
71 emission uncertainties can support atmospheric observation system design, for example for inverse modelling  
72 studies. An ensemble of model runs can represent the spread in atmospheric concentration fields due to the  
73 uncertainty in emissions. Locations with a large spread in atmospheric concentrations are most sensitive to  
74 uncertainties in the emission inventory and are preferential locations for additional atmospheric measurements.  
75 To conclude, emission uncertainties are a critical part of emission verification systems and require more attention.  
76 To better understand how uncertainties in underlying data affect the overall uncertainty in gridded emissions, a  
77 family of ten emission inventories is compiled within the H2020-project CO<sub>2</sub> Human Emissions (CHE) project,  
78 which is funded by the Horizon 2020 EU Research and Innovation programme (see Data Availability). ~~These can~~  
79 ~~be made available upon request.~~ The methodology used to create this family of emission inventories also forms  
80 the basis for the work described here.

81 In this paper we illustrate a statistically coherent method to assess the uncertainties in a high-resolution emission  
82 inventory, including uncertainties resulting from spatiotemporal disaggregation. For this purpose, we use a Monte  
83 Carlo simulation to propagate uncertainties in underlying parameters into the total uncertainty in emissions (like  
84 the Tier 2 approach). We illustrate our methodology using a new high-resolution emission inventory for a  
85 European ~~zoom~~-region centred over the Netherlands and Germany (Table 1). We illustrate the magnitude of the  
86 uncertainties in emissions and how this affects simulated concentrations. The research questions are:

- 87 1) How large are uncertainties in total inventory emissions and how does this differ per sector and country?
- 88 2) How do uncertainties in spatial proxy maps affect local measurements?
- 89 3) How important is the uncertainty in ~~time-temporal~~ profiles for the calculation of annual emissions from  
90 daytime (12-16h LT) emissions, which result from urban inverse modelling studies using only daytime  
91 observations?
- 92 4) What information can we gain from high-resolution gridded uncertainty maps by comparing different  
93 regions?

94 Inverse modelling studies often focus on a single species like CO<sub>2</sub>, but co-emitted species are increasingly  
95 included to allow source partitioning-apportionment (Boschetti et al., 2018; Zheng et al., 2019). In this study, we  
96 look into CO<sub>2</sub> and CO to illustrate our methodology, but the methodology can be applied to other (co-emitted)  
97 species.

## 98 2 Methodology

### 99 2.1 The high-resolution emission inventory

100 **Table 1: Characteristics of the high-resolution emission inventory TNO GHGco v1.01 containing fossil fuel (FF) and**  
101 **biofuel (BF) emissions.**

---

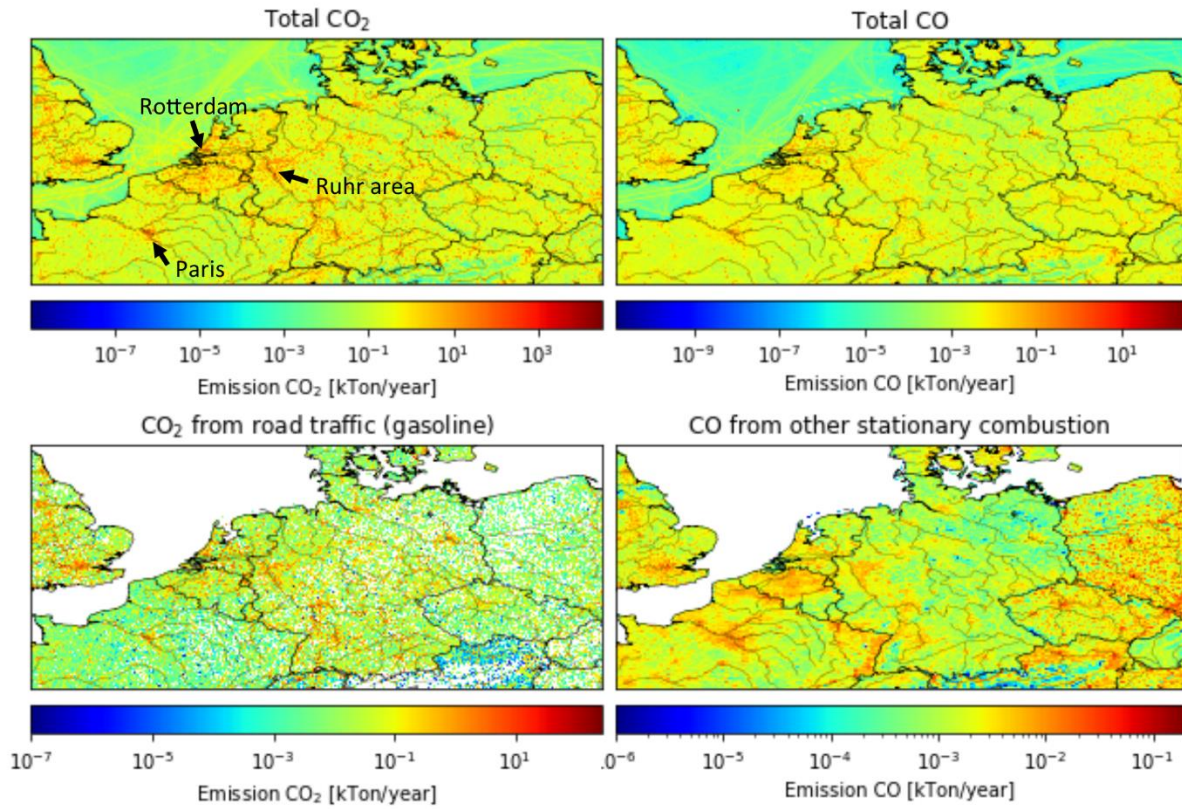
<b>Air pollutants</b>	<u>FFCO<sub>2</sub></u> , <u>BFCO<sub>2</sub></u> , NO <sub>x</sub>
<b>Greenhouse gases</b>	<u>FFCO<sub>2</sub></u> , <u>BFCO<sub>2</sub></u> , CH <sub>4</sub>
<b>Resolution</b>	1/60° longitude x 1/120° latitude (~ 1x1 km over central Europe)
<b>Period covered</b>	2015 (annual emissions)
<b>Domain</b>	-2° W–19° E, 47° N–56°N
<b>Sector aggregation</b>	GNFR (A to L), with GNFR F (Road Transport) split in F1 to F4 (total 16 sectors)
<b>Countries</b>	Complete: <u>Germany, Netherlands, Belgium, Luxembourg, Czech Republic</u> <u>DEU,</u> <u>NLD, BEL, LUX, CZE</u> Partially: <u>United Kingdom, France, Denmark, Austria, Poland, Switzerland, Italy,</u> <u>Slovakia and Hungary</u> <u>GBR, FRA, DNK, AUT, POL, CHE, ITA, SVK and HUN</u>

---

102

103 The basis of this study is a high-resolution emission inventory for the greenhouse gases CO<sub>2</sub> and CH<sub>4</sub> and the co-  
104 emitted tracers CO and NO<sub>x</sub> for the year 2015 (TNO GHGco v1.0, see details in Table 1). In this paper we only  
105 use CO<sub>2</sub> and CO, which are divided over fossil fuel (FF) and biofuel (BF) emissions (no land use and land use  
106 change emissions are included). The emission inventory covers a domain over Europe, including Germany,  
107 Netherlands, Belgium, Luxembourg and the Czech Republic, and parts of Great Britain, France, Denmark, Austria  
108 and Poland (see also Figure 1).

109 The emission inventory is based on the reported emissions by European countries to the UNFCCC (only  
110 greenhouse gases) and to EMEP/CEIP (European Monitoring and Evaluation Programme/Centre on Emission  
111 Inventories and Projections, only air pollutants). UNFCCC CO<sub>2</sub> emissions have been aggregated to ~250 different  
112 combinations of NFR sectors (Nomenclature For Reporting) and fuel types. EMEP/CEIP CO emissions have been  
113 split over the same NFR sector-fuel type combinations by TNO using the GAINS model (Amann et al., 2011)  
114 and/or TNO data. In some cases, the reported data was gap-filled, or replaced ~~or (dis)aggregated with emissions~~  
115 from the GAINS model, EDGAR inventory or internal TNO estimates to obtain a consistent dataset. Next, each  
116 NFR sector is linked to a high-resolution proxy map (e.g. population density for residential combustion of fossil  
117 fuels or AIS (Automatic Identification System) data for shipping re-gridded to 1/60° x 1/120°), which is used to  
118 spatially disaggregate the reported country-level emissions. Where possible, the exact location and reported  
119 emission of large point sources is used (e.g. from the E-PRTR (European Pollutant Release and Transfer  
120 Register)). The third step is temporal disaggregation, for which standard ~~time-temporal~~ profiles are used (Denier  
121 van der Gon et al., 2011). Finally, the ~~gridded~~ emissions are aggregated ~~per-to~~ GNFR (gridded NFR) sectors (see  
122 Table 2) for the emission inventory. The final emission maps of CO<sub>2</sub> and CO are shown in Figure 1, together with  
123 two examples of a source sector map. Note that these maps do not clearly show the large point source emissions,  
124 while these make up almost 45 % of all CO<sub>2</sub> emissions and 26 % of all CO emissions.



125

126 **Figure 1: Total emissions of CO<sub>2</sub> and CO, road traffic (gasoline) emissions of CO<sub>2</sub>, and other stationary combustion**  
 127 **emissions of CO for 2015 in kt yr<sup>-1</sup> (defined per grid cell).**

128 **2.2 Uncertainties in parameters**

129 The emission inventory is used as basis for an uncertainty analysis by assigning an uncertainty to each parameter  
 130 underlying the UNFCCC-EMEP/CEIP emission inventories and further disaggregation thereof. Although the  
 131 aggregation to GNFR sectors makes the emission inventory more comprehensible, we use the more detailed  
 132 underlying data for the uncertainty analysis. The reason is that the uncertainties can vary enormously between  
 133 sub-sectors and fuel types. Generally, the emission at a certain time and place is determined by four types of  
 134 parameters: activity data, emission factor, spatial distribution and time-temporal profile. The activity data and  
 135 emission factors are used by countries to calculate their emissions. The spatial proxy maps and time-temporal  
 136 profiles are used for spatiotemporal disaggregation. All uncertainties need to be specified per NFR sector-fuel  
 137 type combination that is part of the Monte Carlo simulation. In the following sections the steps taken to arrive at  
 138 a covariance matrix for the Monte Carlo simulation are described. Tables with uncertainty data can be found in  
 139 the Appendix A.

140 **Table 2: Overview of aggregated NFR (GNFR) sectors distinguished in the emission inventory**

GNFR category	GNFR category name
A	A_PublicPower
B	B_Industry
C	C_OtherStationaryComb
D	D_Fugitives
E	E_Solvents



<b>F</b>	F_RoadTransport
<b>F1</b>	F_RoadTransport_exhaust_gasoline
<b>F2</b>	F_RoadTransport_exhaust_diesel
<b>F3</b>	F_RoadTransport_exhaust_LPG_gas
<b>F4</b>	F_RoadTransport_non-exhaust
<b>G</b>	G_Shipping
<b>H</b>	H_Aviation
<b>I</b>	I_OffRoad
<b>J</b>	J_Waste
<b>K</b>	K_AgriLivestock
<b>L</b>	L_AgriOther

---

### 141 **2.2.1 Parameter selection**

142 The first step is to identify which parameters should be included in the Monte Carlo simulation. As mentioned  
143 before there are about 250 different combinations of NFR sectors and fuel types and including all of them would  
144 be a huge computational challenge. However, a selection of 112 combinations makes up most of the fossil fuel  
145 emissions (96 % for CO<sub>2</sub> and 92 % for CO) and therefore a pre-selection was made. This results in a covariance  
146 matrix of 224x224 parameters (112 sector-fuel combinations for two species). To further reduce the size of the  
147 problem, the emissions are partly aggregated before starting the Monte Carlo for the spatial proxies (mostly fuels  
148 are combined per sector, because they have the same spatial distribution). This results in a total of 59 NFR sector-  
149 spatial proxy combinations, which are put in a separate covariance matrix. The ~~time-temporal~~ profiles are applied  
150 to the aggregated GNFR sectors, which make up the last covariance matrix. Note that the spatial proxies and ~~time~~  
151 ~~temporal~~ profiles are the same for CO<sub>2</sub> and CO<sub>2</sub>; ~~Only-except for~~ the spatially explicit E-PRTR point source data  
152 can have a different spatial distribution for CO<sub>2</sub> and CO, but they also use the same temporal profiles.

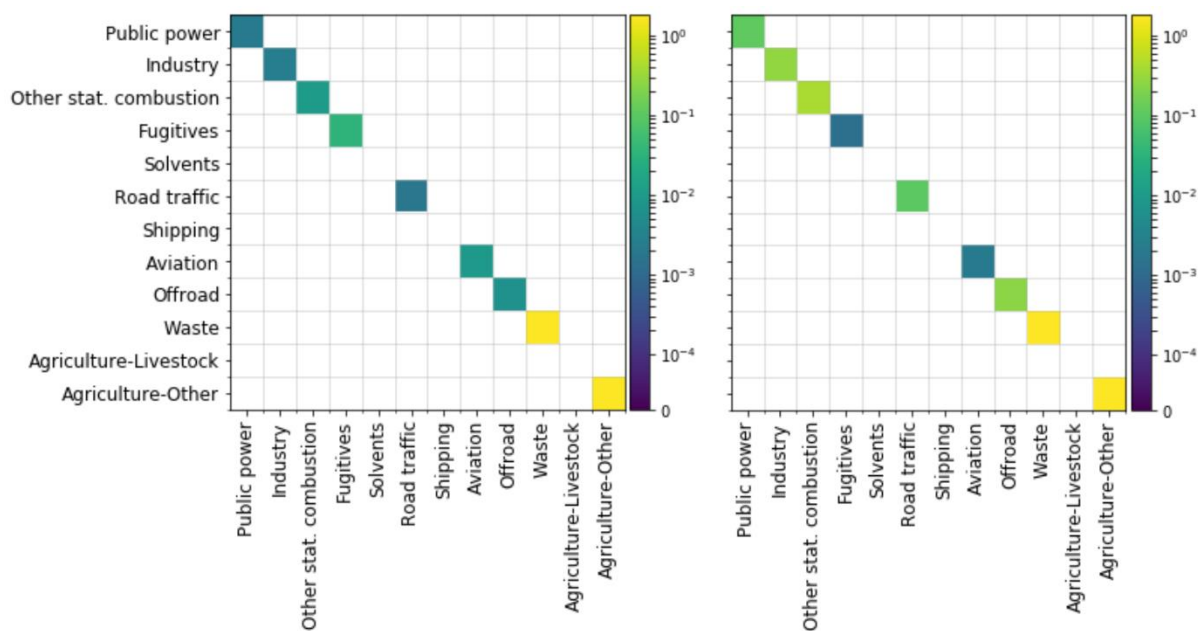
### 153 **2.2.2 Uncertainties in reported emissions**

154 Country-level emissions are estimated from the multiplication of activity data and emission factors. Activity data  
155 consist for the most part of fossil fuel consumption data available from national energy balances. Some fuel  
156 consumptions are better known than others and uncertainties vary across sectors. An emission factor is the amount  
157 of emission that is produced per unit of activity (e.g. amount of fuel consumed). For CO<sub>2</sub> this depends mainly on  
158 the carbon content of the fuel. In contrast, CO emissions are extremely dependent on combustion conditions,  
159 ~~ertain-choice of~~ industrial processes and in-place technologies.

160 The NIR's for greenhouse gases (GHGs) provide a table with uncertainties in activity data and CO<sub>2</sub> emission  
161 factors on the level of NFR sector - fuel combinations. The uncertainties reported by each country are averaged  
162 to get one uncertainty per NFR sector-fuel combination for the entire domain. Overall, the differences in reported  
163 uncertainties between countries are small. The uncertainties in activity data and CO<sub>2</sub> emission factors are relatively  
164 low and normally distributed.

165 The CO emission factors are mostly based on ~~basic~~ uncertainty ranges provided in the EMEP/EEA Guidebook  
166 (European Environment Agency, 2016) and supplemented by BAT reference documents from which reported  
167 emission factor ranges are taken as uncertainty range (<http://eippcb.jrc.ec.europa.eu/reference/>). The CO emission

168 factor uncertainties are generally expressed by a factor, which means that the highest and lowest limit values are  
 169 either the specified factor above or below the most common value. Therefore, these uncertainties have a lognormal  
 170 distribution and are relatively large.



171  
 172 **Figure 2: Covariance matrices for total emissions of CO<sub>2</sub> (left) and CO (right) per aggregated source sector. A white**  
 173 **space on the diagonal indicates this sector is not included in the Monte Carlo simulation.**

174 To estimate the overall uncertainty in the emissions per NFR sector-fuel combination, the uncertainties in the  
 175 activity data and emission factors need to be combined (shown in Figure 2 for the aggregated GNFR sectors).  
 176 When both uncertainties are of the same order and relatively small, as well as both having a normal distribution,  
 177 the overall emission uncertainty is calculated with the standard formula for error propagation for non-correlated  
 178 normally distributed variables (see Sect. 2.4). For most CO emission factors, uncertainties are much higher and  
 179 have a lognormal distribution instead of normal. In that case the uncertainty of the variable with the highest  
 180 uncertainty is assumed to be indicative for the overall uncertainty of the emission, which in general means the  
 181 uncertainty of the CO emission factor determines the overall uncertainty of the CO emission, with the distribution  
 182 remaining lognormal. The error introduced by fuel type disaggregation for CO is not considered.

183 Finally, for power plants and road traffic we assumed error correlations to exist between different sub-sectors per  
 184 fuel type, and between different fuel types per sub-sector for other NFR sectors. In some cases, correlations also  
 185 exist between different NFR sectors belonging to the same GNFR sector. The definition of correlations is  
 186 important, because they affect the total uncertainties. For example, if emission factors of sub-sectors are  
 187 correlated, deviations can amplify each other, leading to higher overall uncertainties. In contrast, the division of  
 188 the well-known total fuel consumption of a sector over its sub-sectors includes an uncertainty which is anti-  
 189 correlated (i.e. if too much fuel consumption is assigned to one sub-sector, too little is assigned to another). This  
 190 has little impact on the total emissions, because uncertainties only exist at lower levels.

### 191 2.2.3 Uncertainties in spatial proxies

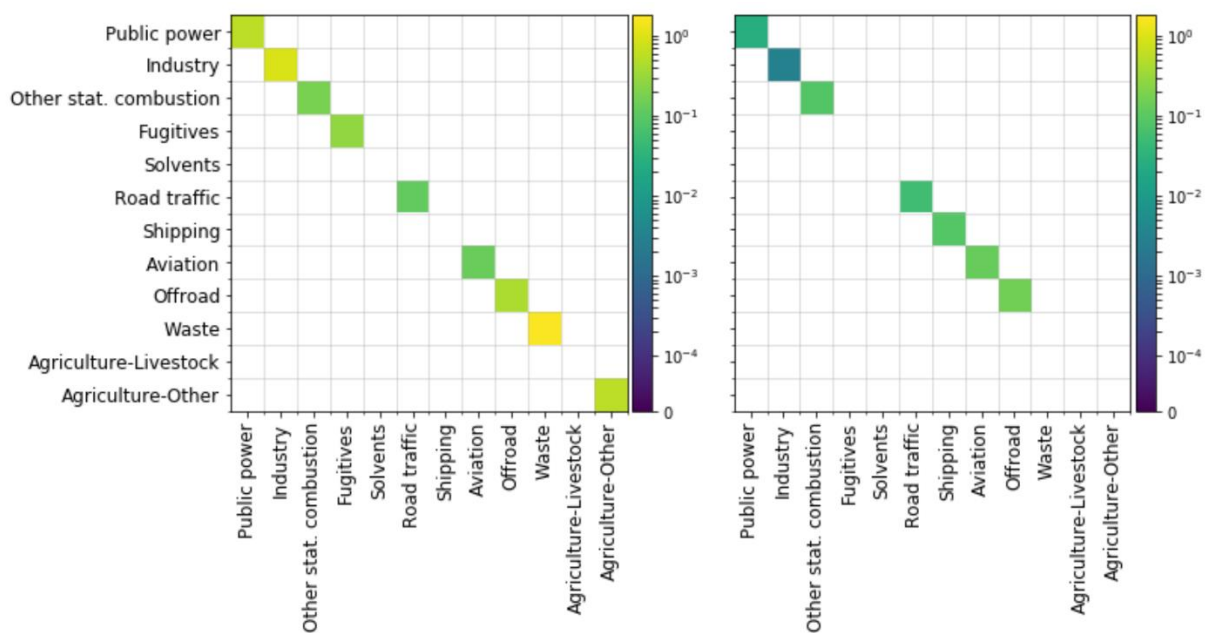
192 The proxy maps used for spatial disaggregation can introduce a large uncertainty coming from the following  
 193 sources:

- 194 1) The proxy is not correctly representing real-world locations of what it is supposed to represent, either  
 195 because there are cells included in which none of the intended activity takes place or cells are missing in  
 196 which the intended activity does take place (proxy quality).  
 197 2) The proxy is not fully representative for the activity it is assumed to represent, for example if there is a non-  
 198 linear relationship between the proxy value and the emission (proxy representativeness): a grid cell with  
 199 twice the population density does not necessarily have double the amount of residential heating emissions,  
 200 because heating can be more efficient in densely populated areas and/or apartment blocks.  
 201 3) The cell values themselves are uncertain, e.g. the population density or traffic intensity (proxy value).

202 We attempt to capture the second and third source of uncertainty in a single numerical indicator representing the  
 203 uncertainty at cell level (see Figure 3 for the uncertainty per aggregated GNFR sector). The overall uncertainties  
 204 are based on expert judgement and inevitably include a considerable amount of subjectivity. This type of  
 205 uncertainty is often large and has a lognormal distribution, except for proxies related to road traffic and some  
 206 proxies related to commercial/residential emissions sources. We assume no error correlations exist. The first  
 207 source of uncertainty is also considered in one of the experiments (see Sect. 2.4 for a description of this  
 208 experiment).

### 209 2.2.4 Uncertainties in ~~time~~-temporal profiles

210 ~~The~~ For each GNFR sector the emission timing is described using three ~~time~~-temporal profiles: one profile that  
 211 describes the seasonal cycle (monthly fractions), one profile that describes the day-to-day variations within a week  
 212 (daily fractions), and one profile that describes the diurnal cycle (hourly fractions). ~~currently consist of fixed~~  
 213 ~~monthly, daily and hourly fractions~~ These profiles ~~that~~ are based on long-term average activity data and/or socio-  
 214 economic characteristics ~~and~~. These profiles ~~are~~ applied for each year and for the entire domain, considering only  
 215 time zone differences. In reality, the ~~time~~-temporal profiles can differ between countries, ~~and~~ from year to year  
 216 ~~and the diurnal cycle can vary between weekdays and weekends~~. For example, residential emissions are strongly  
 217 correlated with the outside temperature, ~~which follows a different pattern each year~~. ~~and therefore show a strong~~  
 218 ~~seasonal cycle. However, one winter can be very cold, whereas the next can have above average temperatures.~~



219

220 **Figure 3: Covariance matrices for spatial proxies (left) and time profiles (right) per aggregated source sector. These**  
 221 **are the same for CO<sub>2</sub> and CO. A white space on the diagonal indicates this sector is not included in the Monte Carlo**  
 222 **simulation.**

223 To quantify the uncertainty in time-temporal profiles, a range of time-temporal profiles (for a full year, hourly  
 224 resolution) was created for each source sector based on activity data (such as traffic counts). These profiles can  
 225 be from different years and countries, so that the full range of possibilities is included. These are compared to the  
 226 fixed time-temporal profiles to estimate the uncertainties, which are normally distributed (see Figure 3 for the  
 227 uncertainty per aggregated GNFR sector). We assume no error correlations exist.

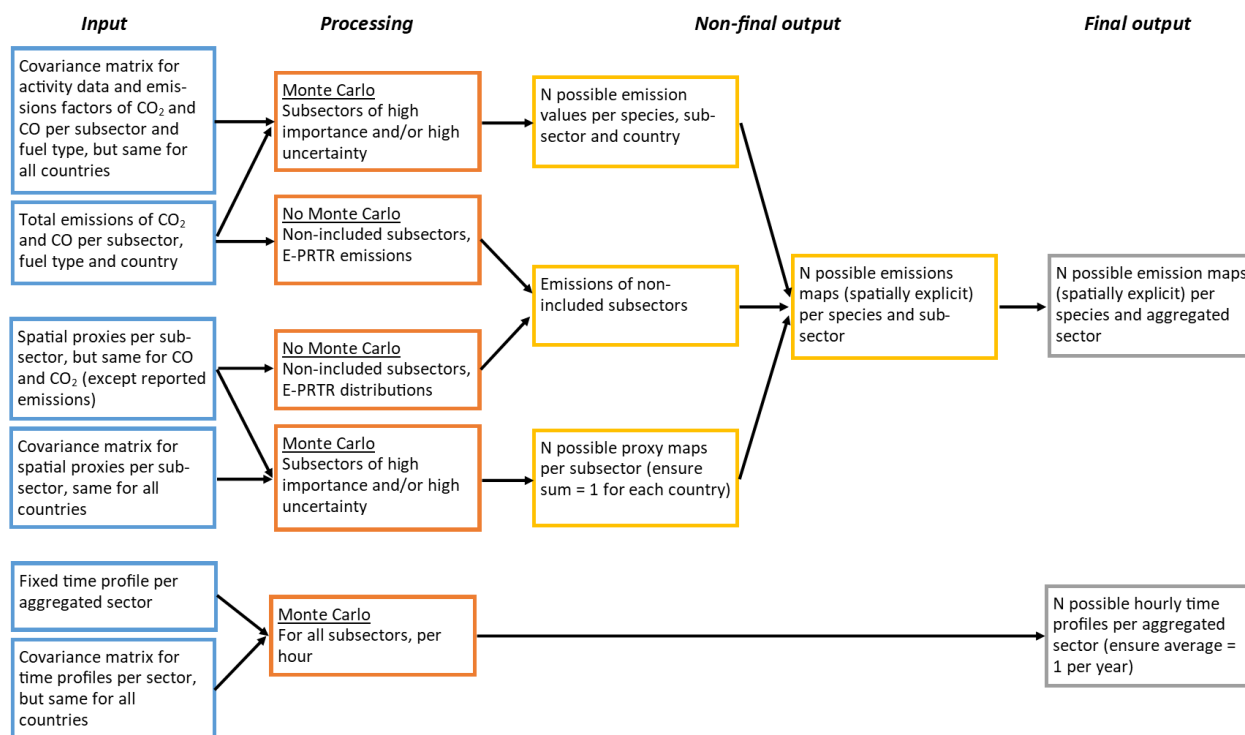
228 **Table 3: Percentage (%) of emissions of CO<sub>2</sub> and CO (fossil + biofuel<sub>FF</sub> + BF) that are attributed to large point sources**  
 229 **(accounted for in databases) for source sectors public power and industry.**

Country	CO <sub>2</sub>		CO	
	Public power	Industry	Public power	Industry
Netherlands	84.3 %	80.4 %	80.7 %	86.0 %
Belgium	65.4 %	77.5 %	99.5 %	93.5 %
Luxembourg	67.1 %	67.2 %	61.8 %	94.2 %
Germany	85.9 %	74.1 %	96.7 %	87.9 %
Czech Republic	89.2 %	90.4 %	79.3 %	94.3 %

### 230 2.3 The Monte Carlo simulation

231 Within a Monte Carlo simulation we create an ensemble (size N) of emissions, spatial proxies and time-temporal  
 232 profiles by drawing random samples from the covariance matrices described in Sect. 2.2. This creates a set of  
 233 possible solutions in the emission space, reflecting the uncertainties in the underlying parameters. The entire  
 234 process is shown in Figure 4. As mentioned before, not all sub-sectors are included in the Monte Carlo simulation  
 235 and the non-included emissions are added to each ensemble member at the final stage. It is important to ensure  
 236 that the time-temporal profiles and the spatial proxies do not affect the total emissions, so proxies should sum up  
 237 to 1 for each country and time-temporal profiles should be on average 1 over a full year. Before doing this, negative  
 238 values are removed.

239 The source sectors that include point source emissions (mainly public power and industry) are treated separately.  
 240 The large point source emissions and their locations are relatively well-known and available from databases (e.g.  
 241 from E-PRTR), and therefore not included in the Monte Carlo. The remaining part of the emissions (non-point  
 242 source or small point sources) from these sectors are distributed using generic proxies (e.g. industrial areas) and  
 243 are calculated as the difference between the total emissions (activity data x emission factor) and the sum of the  
 244 point source emissions. If negative emissions result from this subtraction of reported point source emissions, the  
 245 residual is set to zero. Note that the spatial uncertainty of this residual part is often high. The fraction of the public  
 246 power and industrial emissions that are attributed to large point sources are shown in Table 3 for several countries.



247

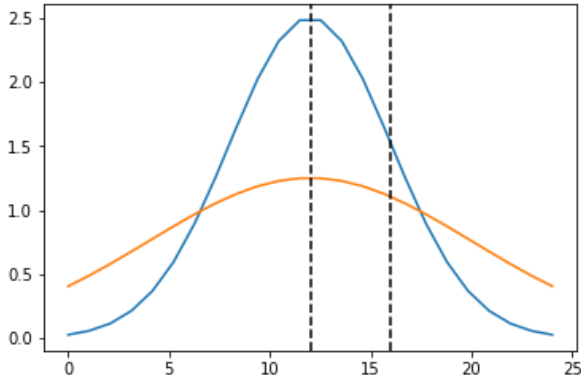
248 **Figure 4: Flow-diagram showing the input, processing and output of the Monte Carlo simulation.**

## 249 2.4 Experiments to explore uncertainty propagation

250 In this paper several experiments are performed to examine the impact of the uncertainties in different parameters  
 251 on the overall emissions and simulated concentrations:

- 252 1) The first experiment uses a Monte Carlo simulation (N=500) to illustrate the spread in emissions per sector  
 253 due to uncertainties in emission factors and activity data (no spatial/temporal variability is considered). This  
 254 sample size is based on an analysis of the robustness of the uncertainty estimate (Janssen, 2013), which  
 255 shows that a sample size of 500 is sufficient to get robust results (Appendix B). This experiment is used to  
 256 show the contribution of specific sectors to the overall uncertainty and to illustrate how uncertainties vary  
 257 between sectors and countries. For this experiment country totals are used, also for the countries that are  
 258 partially outside the zoom domain shown in Figure 1. The results are presented in Sect. 3.1.
- 259 2) The second experiment uses a Monte Carlo simulation (N=500) to illustrate how the uncertainty in spatial  
 260 proxy maps is translated into uncertainties in simulated concentrations (emissions are taken constant; no  
 261 temporal variability is included). We use emissions of other stationary combustion (CO<sub>2</sub>) and road traffic  
 262 (CO) to illustrate the importance of having a correct spatial distribution for measurements close to the source  
 263 area and further away. The results are presented in Sect. 3.2.
- 264 3) The third experiment compares two spatial proxy maps for distributing ‘residual’ power plant emissions  
 265 (i.e. those not accounted for in point source databases) to illustrate the potential impact of spreading out  
 266 small point source emissions when zooming in on small case study areas (emissions are taken constant; no  
 267 temporal variability is included). The results are presented in Sect. 3.2.
- 268 4) The fourth experiment uses a Monte Carlo simulation (N=500) to illustrate the spread in time-temporal  
 269 profiles (emissions are taken constant; no spatial variability is considered). We use this information to  
 270 determine the error introduced when extrapolating daytime (12–16 h LT) emissions (for example resulting

271 from an inversion) to annual emissions using an incorrect time-temporal profile. Figure 5 shows two  
 272 possible daily cycles, which have 46 % (blue) and 25 % (orange) of their emissions between 12 and 16 h  
 273 LT. Therefore, both time-temporal profiles will give a different total daily emission when used to extrapolate  
 274 derive the daytime emissions. The results are presented in Sect. 3.3.



275  
 276 **Figure 5: Schematic overview of two possible time-temporal profiles, which represent a different fraction of the total**  
 277 **daily emissions during the selected period (12–16 h LT, illustrated by the dashed lines).**

278 5) For the final experiment, maps are made of the (absolute and relative) uncertainty in each pixel, including  
 279 uncertainties in emission factors, activity data and spatial proxies (no temporal variability). For this we used  
 280 a Tier 1 approach, using the following equations:

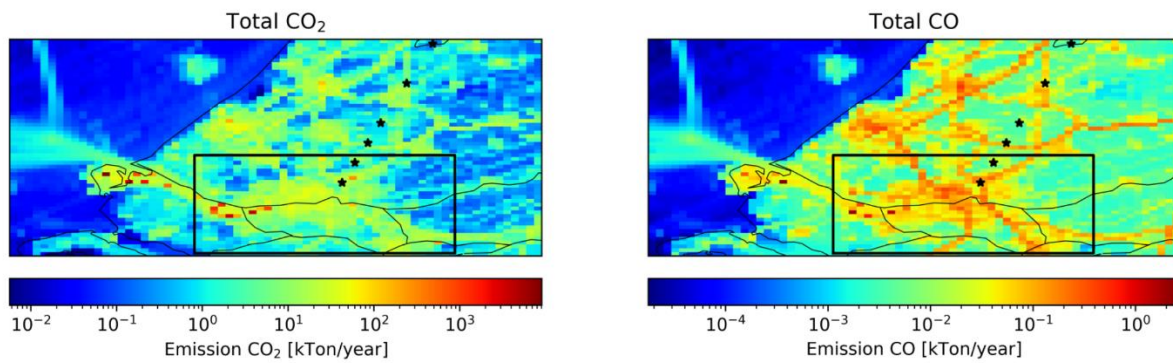
281 
$$\text{Total relative uncertainty} = \sqrt{\sum \text{standard deviations}^2} / \text{emission sum} \quad (1)$$

282 for the summation of uncorrelation quantities (e.g. sectoral emissions), and:

283 
$$\text{Total relative uncertainty} = \sqrt{\sum \text{relative uncertainties}^2} \quad (2)$$

284 for the multiplication of random variables, such as used to combine activity data and emission factors. Here,  
 285 the (total) relative uncertainty is the percentage uncertainty (uncertainty divided by the total) and the  
 286 standard deviations are expressed in units of the uncertain quantity (percentage uncertainty multiplied with  
 287 the uncertain quantity). These maps are used to explore spatial patterns in uncertainties and examine what  
 288 we can learn about different countries or regions. The results are presented in Sect. 3.4.

289 For experiment 2 and 3 a smaller domain is selected to represent a local case study (Figure 6). We used the  
 290 Rotterdam area, which has been studied in detail before (Super et al., 2017b, 2017a). The domain is about 34x26  
 291 km and centred over the city, which includes some major industrial activity as well. To translate the emissions  
 292 into atmospheric concentrations, a simple plume dispersion model is used, the Operational Priority Substances  
 293 (OPS) model. This model was developed to calculate the transport of pollutants, including chemical  
 294 transformations (Van Jaarsveld, 2004; Sauter et al., 2016) and was adapted to include CO and CO<sub>2</sub> (Super et al.,  
 295 2017a). The short-term version of the model calculates hourly concentrations at specific receptor points,  
 296 considering hourly variations in wind direction and other transport parameters. Although the model is often used  
 297 for point source emissions, it can also handle surface area sources. This model was chosen because of its very  
 298 short run time, which makes it suitable for a large ensemble. The model is run for each of the alternative emission  
 299 maps.



300

301 **Figure 6: Emissions of CO<sub>2</sub> (left) and CO (right) for part of the Netherlands, including the sub-domain (black rectangle)**  
 302 **over Rotterdam. Black stars indicate the receptor locations.**

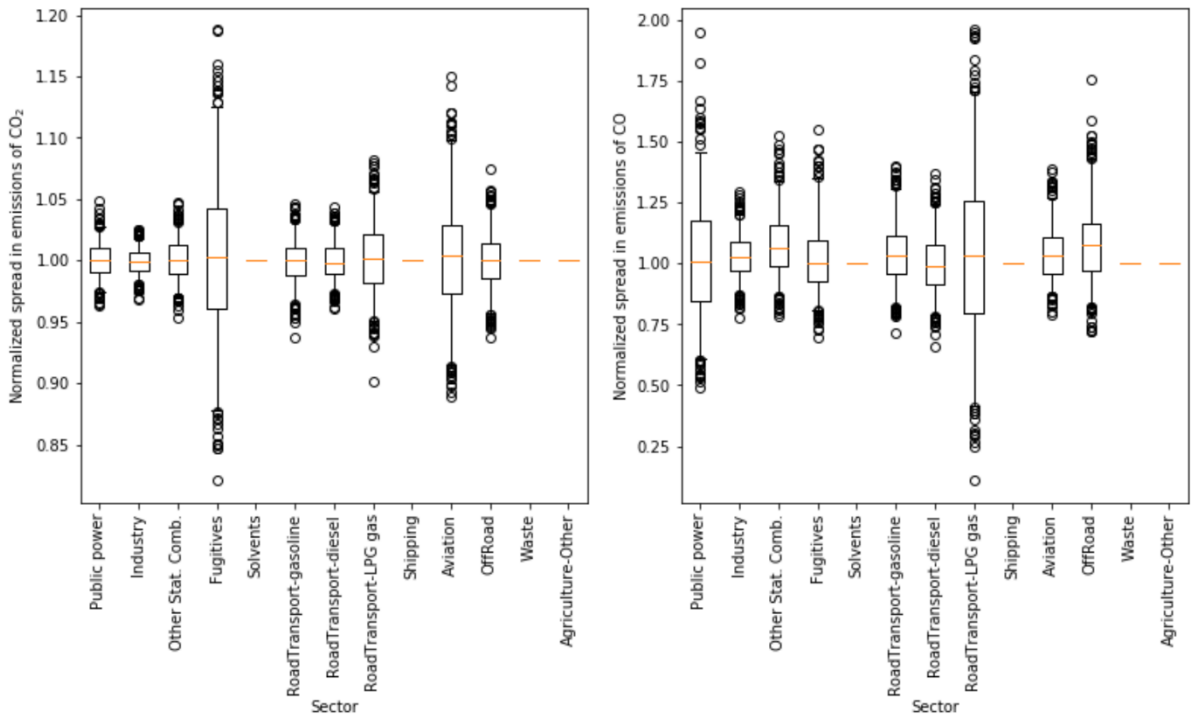
303 The OPS model is run for each ensemble member for 5 January 2014 from the start of the day until 16 h LT. On  
 304 this day the wind direction is relatively constant at about 215° and the wind speed is around 6 m s<sup>-1</sup>. We specify  
 305 receptor points downwind from the centre of our domain at increasing distance (5, 10, 15, 20, 30 and 40 km). We  
 306 use the last hour of the simulation for our analyses. We assume emissions from other stationary combustion and  
 307 road traffic (experiment 2) to take place at the surface. The initial emissions of ‘residual’ power plants, smeared  
 308 out over all industrial areas, are also emitted at the surface. However, we raise the height of the emissions to 20m  
 309 when these emissions are appointed to specific pixels. This height is representative for stack heights of small  
 310 power plants.

### 311 3 Results

#### 312 3.1 Uncertainties in total emissions

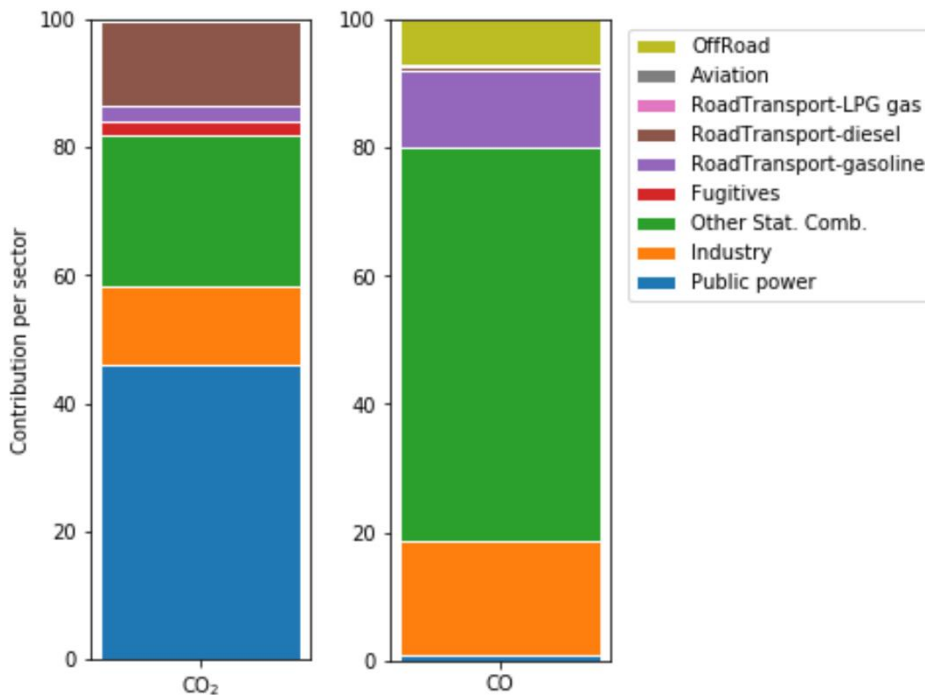
313 Using the uncertainties in emission factors and activity data we can evaluate the uncertainty in the total emissions  
 314 of CO<sub>2</sub> and CO per sector. Figure 7 shows the normalized spread in emissions per sector based on the Monte Carlo  
 315 simulation (N=500). The CO<sub>2</sub> emissions have a relatively small uncertainty range and the uncertainty in the total  
 316 emissions (all sectors together if we sum all emissions for each of the 500 solutions) is only about 1 % (standard  
 317 deviation). The largest uncertainties are for fugitives and aviation, which are only small contributors to the total  
 318 CO<sub>2</sub> emissions (1.3 % and 0.4 %, respectively). Therefore, their contribution to the total emission uncertainty is  
 319 very small, as is shown in Figure 8. The largest uncertainty in the total CO<sub>2</sub> emissions is caused by the public  
 320 power sector. Despite the relatively small uncertainty in the emissions from this sector, it is the largest contributor  
 321 to the total CO<sub>2</sub> emissions (33 %) and therefore the uncertainty in the public power sector contributes about 45 %  
 322 to the uncertainty in the total CO<sub>2</sub> emissions.

323 In contrast, the CO emissions show a larger uncertainty bandwidth with many high outliers caused by the  
 324 lognormal distribution of uncertainties in the emission factors. The uncertainty in the total emissions is 6 % for  
 325 CO (standard deviation). Here, again the largest uncertainties are related to sectors (public power and road  
 326 transport (LPG fuel)) that are relatively small contributors to the total CO emissions. The main contributor to the  
 327 uncertainty in total CO emissions is other stationary combustion, which contributes about 31 % to the total  
 328 emissions and is responsible for more than 60 % of the total uncertainty.



329

330 **Figure 7: Normalized spread in emissions of CO<sub>2</sub> (left) and CO (right).** The box represents the interquartile range, the  
 331 whiskers the 2.5–97.5 percentile, the lines the median values, and the circles are outliers. For sectors where no box is  
 332 drawn there is no data included in the Monte Carlo simulation. Note the different scales of the y-axis.



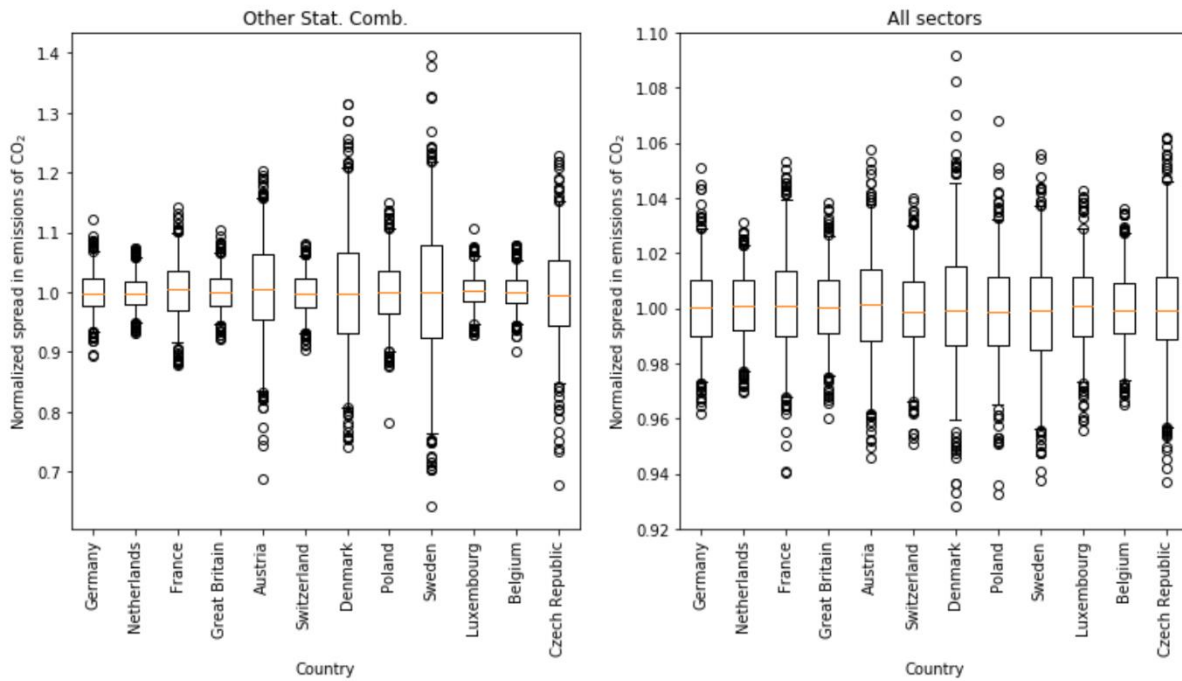
333

334 **Figure 8: Contribution of source sectors to the total uncertainty in CO<sub>2</sub> (left) and CO emissions (right), summing to**  
 335 **100 %.**

336 Although the uncertainty in each parameter is assumed to be the same for each country, how a sector is composed  
 337 of sub-sectors can vary per country. Therefore, the uncertainty per aggregated sector can also vary per country.  
 338 An example is shown in Figure 9 (left panel), which shows the normalized spread in CO<sub>2</sub> emissions of other  
 339 stationary combustion for all countries within the domain. We find a much larger uncertainty in countries where



340 the relative fraction of biomass combustion is larger, because biomass burning has a much larger uncertainty in  
 341 both the activity data and the emission factor. For example, the percentage of biomass burning in the residential  
 342 sector is 54 % for the Czech Republic and 65 % for Denmark, compared to only 11 % and 9 % for the Netherlands  
 343 and Great Britain. Thus, differences in the fuel composition of countries result in differences in the overall  
 344 emission uncertainties, even if the uncertainty per parameter is estimated to be the same. Overall For the total CO<sub>2</sub>  
 345 emissions, the differences between countries are relatively small, with standard deviations between 1.2 and 2.3 %  
 346 (Figure 9, right panel).



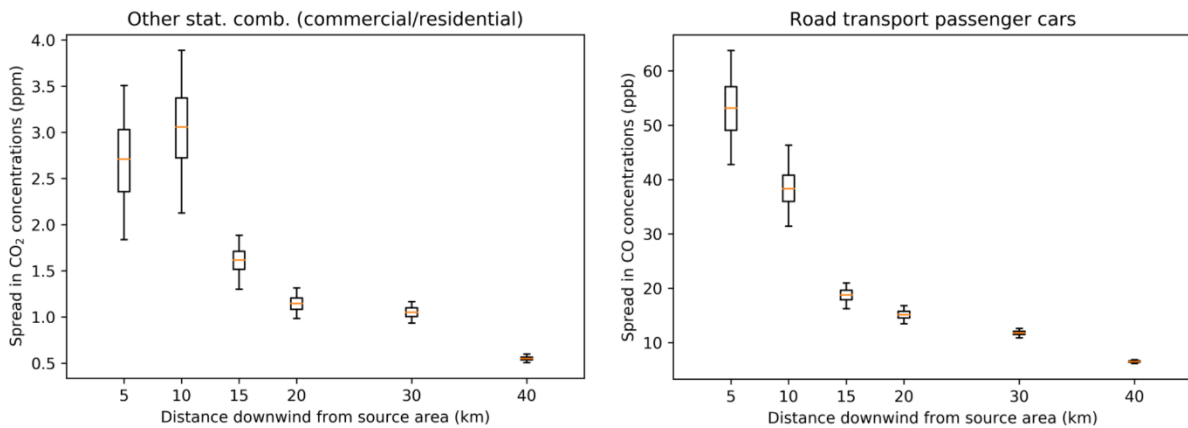
347  
 348 **Figure 9: Normalized spread in emissions of CO<sub>2</sub> for other stationary combustion (left) and all sectors combined (right)**  
 349 **for a range of countries. The box represents the interquartile range, the whiskers the 2.5–97.5 percentile, the lines the**  
 350 **median values, and the circles are outliers.**

### 351 3.2 Uncertainties in spatial proxies

352 We examined the impact of uncertainties in spatial proxies on modelled CO<sub>2</sub> and CO concentrations for major  
 353 source sectors. For CO<sub>2</sub> we selected other stationary combustion (only commercial/residential, no  
 354 agriculture/forestry/fishing). The largest fraction (>90 %) of CO<sub>2</sub> emissions from this sector is distributed using  
 355 population density as proxy, which is used here (the remainder of the emissions is not considered). The uncertainty  
 356 in this sector-proxy combination is estimated to be 50% (normal distribution), mainly due to the disaggregation  
 357 to the 1x1 km resolution. For CO we selected road transport (all fuels, but only passenger cars). The spatial proxy  
 358 for distributing passenger car emissions is based on traffic intensities compiled using Open Transport Map and  
 359 Open Street Map, vehicle emission factors per road type/vehicle type/country, and fleet composition. The  
 360 uncertainty in this proxy is estimated to be 30 % (normal distribution) due to a higher intrinsic resolution.

361 Figure 10 shows the resulting spread in atmospheric concentrations as a function of downwind distance from the  
 362 source area. Note that the concentrations are enhancements caused by local emissions of the selected source  
 363 sectors and do not include ambient concentrations or other sources. For CO<sub>2</sub> (left panel) we see a concentration  
 364 of about 3.0 ppm at 10 km from the source area centre, but with a large uncertainty bandwidth. This signal is large  
 365 enough to measure, but with this large uncertainty such measurements are difficult to use in an inversion. The

366 measurement at 5 km from the source area centre is slightly lower than the one at 10 km, because it is updownwind  
 367 of a part of the emissions. At longer distances, the magnitude of the atmospheric signal concentration enhancement  
 368 decreases drastically, and so does the absolute spread in concentrations. The signal enhancement becomes too  
 369 small compared to the uncertainties occurring in a regular inversion framework to be useful. The right panel shows  
 370 a similar picture for the CO concentrations resulting from passenger car emissions. Again, the spread in  
 371 concentrations is large close to the source area centre and decreases with distance, but also the magnitude of the  
 372 signal absolute concentration enhancement decreases. However, in this case the concentration at 5 km from the  
 373 source area centre is larger, because it is very close to an emission hot spot (see also Fig. 6). Note that we focus  
 374 here on a single source sector and the overall signals enhancements will be larger and therefore easier to use.  
 375 Nevertheless, the large spread in concentrations shows that a good representation of the spatial distribution is  
 376 important for constraining sectoral emissions.

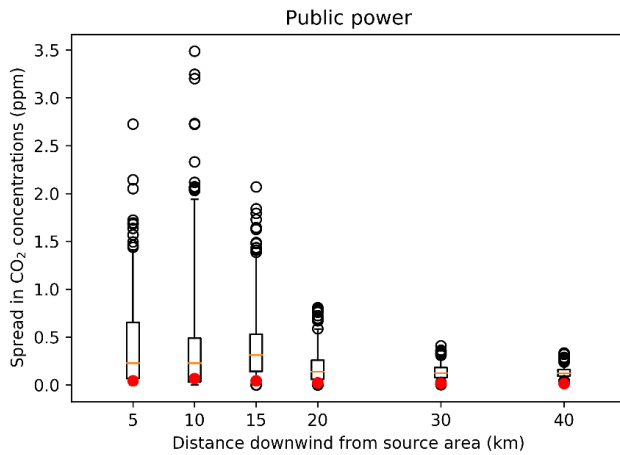


377  
 378 **Figure 10: Spread in simulated concentrations of CO<sub>2</sub> resulting from commercial/residential emissions due to**  
 379 **uncertainties in the total population proxy map (left) and spread in concentrations of CO resulting from road transport**  
 380 **(passenger cars) emissions due to uncertainties in the passenger cars proxy map (right). The box represents the**  
 381 **interquartile range, the whiskers the 2.5–97.5 percentile, and the lines the median values of the full ensemble.**

382 Both proxy maps discussed here are the main proxy maps for the selected sectors. As mentioned before, some  
 383 sectors have residual emissions that are distributed using an alternative proxy map. An example is public power.  
 384 Large power plants are listed in databases, including the reported emissions (Table 3). The remainder of the  
 385 country emissions is spatially distributed over all industrial areas. However, it is more likely that the residual  
 386 emissions should be attributed to specific point sources (small power plants not listed in databases). That means  
 387 that instead of spreading the emissions over a large area, leading to very small local emissions and a low  
 388 concentration gradient, there could be relatively large emissions at a few locations. Therefore, the uncertainty in  
 389 these sector-proxy combinations is assumed to have a lognormal distribution, in part because of the absence of a  
 390 better estimation.

391 We illustrate the effect of this assumption by creating a new proxy map for residual (small) power plants. We find  
 392 that for the Netherlands a total capacity of 3655 MWe by 676 combustion plants is not included as a point source  
 393 (source: S&P Global Platts World Electric Power Plants database (<https://www.spglobal.com/platts/en/products-services/electric-power/world-electric-power-plants-database>)). At least 70 % of this capacity, attributed to 280  
 394 plants, is assumed to be in industrial areas. Given 4052 grid cells designated as industrial area in the Netherlands,  
 395 this is just 7 % of the total amount of industrial area grid cells assuming no more than one plant per grid cell. The  
 396 remainder is mainly related to cogeneration plants from glasshouses, which are located outside the industrial areas.  
 397 Therefore, we create a new proxy map for power plants by equally assigning 70 % of the emissions from the  
 398

399 residual power plants to 20 randomly chosen pixels (7 % of the total amount of industrial area pixels in the case  
 400 study area, i.e. the same density as for the Netherlands as a whole). As mentioned before, we also raise the height  
 401 of the emissions from surface level to 20 m, which is a better estimate of the stack height for small power plants.  
 402 The effect on local measurements is large (Figure 11). Instead of measuring a small and constant signal from this  
 403 sector, the assumed presence of small power plants results in measuring occasional large peak concentrations.  
 404 Thus, despite being relatively unimportant at the national level, for local studies the impact of the uncertainty in  
 405 these ‘residual’ proxies can be large.

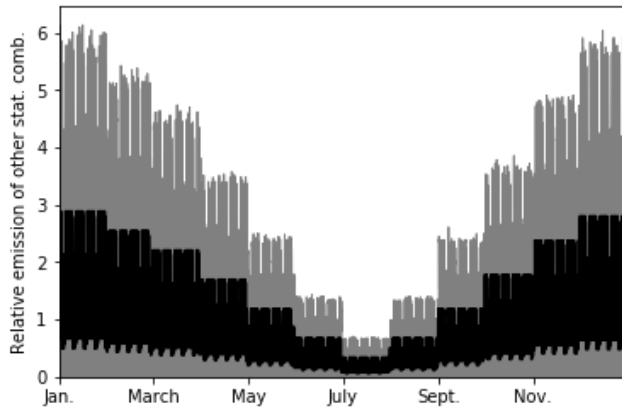


406

407 **Figure 11: Spread in simulated concentrations of CO<sub>2</sub> resulting from public power emissions due to differences in the**  
 408 **proxy map: emissions are distributed using the new proxy map with only 20 randomly chosen pixels containing**  
 409 **emissions. The box represents the interquartile range, the whiskers the 2.5–97.5 percentile, the lines the median values,**  
 410 **and the black circles are outliers of the full ensemble. The red dots show concentrations of CO<sub>2</sub> when the original proxy**  
 411 **map is used (industrial area).**

### 412 3.3 Uncertainties in time-temporal profiles

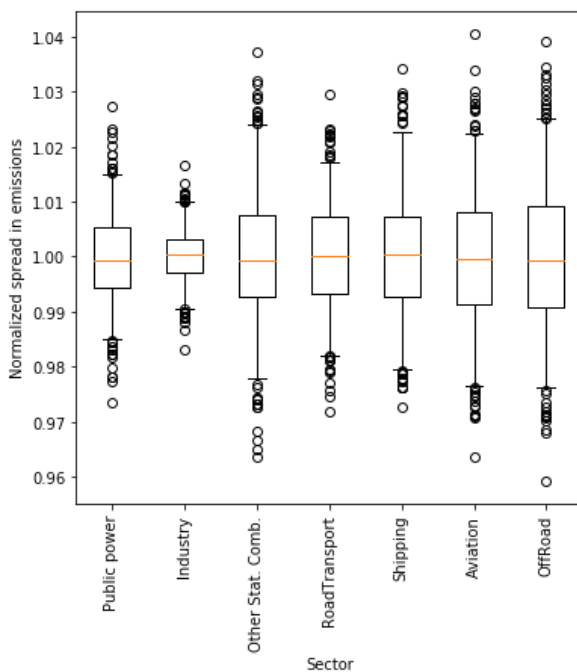
413 The timing of emissions is important to interpret measurements correctly. During morning rush hour, a peak is  
 414 expected in road traffic emissions, but the magnitude of this peak can differ from one day to the next. Also, the  
 415 seasonal cycle in emissions due to heating of buildings can vary between years due to varying weather conditions.  
 416 Yet, often fixed time-temporal profiles are used to describe the temporal disaggregation of annual emissions. The  
 417 range of possible values for the time-temporal profile of other stationary combustion is shown in Figure 12. The  
 418 range can be very large, especially during the winter. However, note that the average of each time-temporal profile  
 419 is 1.0 for a full year, so that the temporally distributed emissions add up to the annual total. Therefore, changes in  
 420 the time-temporal profile indicate shifts in the timing in the emissions and not changes in the overall emissions  
 421 due to cold weather, which are accounted for by the activity data.



422

423 **Figure 12: Spread in time-temporal profiles for other stationary combustion (N=500), resulting from the Monte Carlo**  
 424 **simulation (grey shading). The black line represents the standard time profile.**

425 In inverse modelling, often well-mixed (non-stable) daytime measurements are selected (Boon et al., 2016; Breón  
 426 et al., 2015; Lauvaux et al., 2013), because these are least prone to errors in model transport. For local studies,  
 427 where transport times are short, this means that only afternoon emissions are optimized. The total annual emissions  
 428 can then be calculated using a time-temporal profile. However, if the time-temporal profile is not correct, an  
 429 incorrect fraction of the emissions can be attributed to the selected hours. We examined the impact of using an  
 430 incorrect time-temporal profile on the total yearly emissions by calculating yearly emissions for each ensemble  
 431 member. Figure 13 shows the normalized spread in sectoral emissions for all ensemble members. The error in the  
 432 total annual emissions, resulting from the upscaling of daytime emissions using an incorrect time-temporal profile,  
 433 can reach up to about 1–2 %. This is a significant source of error for country-level CO<sub>2</sub> emissions, but less  
 434 important for CO as the other uncertainties for CO are much larger.



435

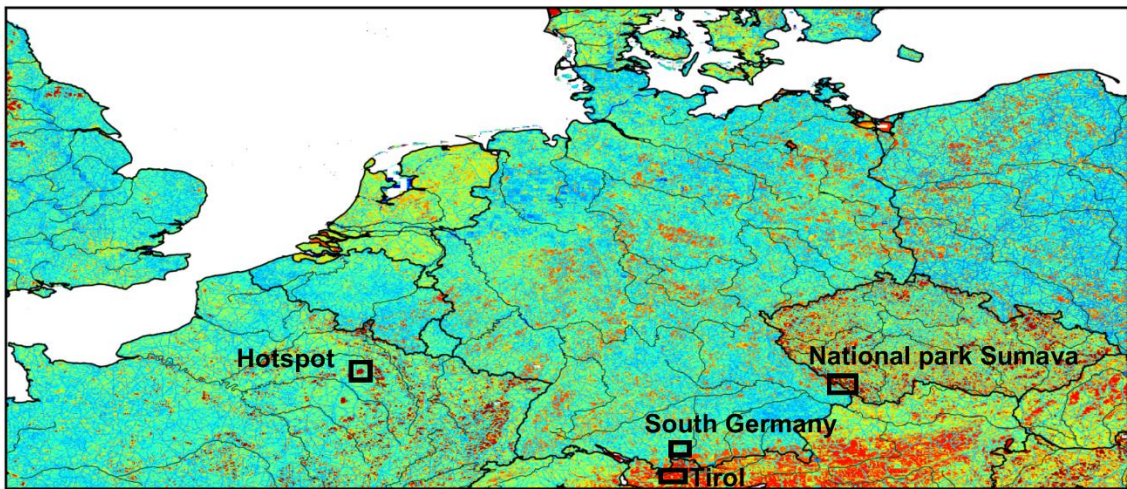
436 **Figure 13: Normalized spread in emissions of CO<sub>2</sub> and CO per sector due to uncertainties in time-temporal profiles.**  
 437 **The box represents the interquartile range, the whiskers the 2.5–97.5 percentile, the lines the median values, and the**  
 438 **circles are outliers. The spread is the same for CO<sub>2</sub> and CO, because they have the same temporal profiles.**

439 **3.4 Uncertainty maps and spatial patterns**

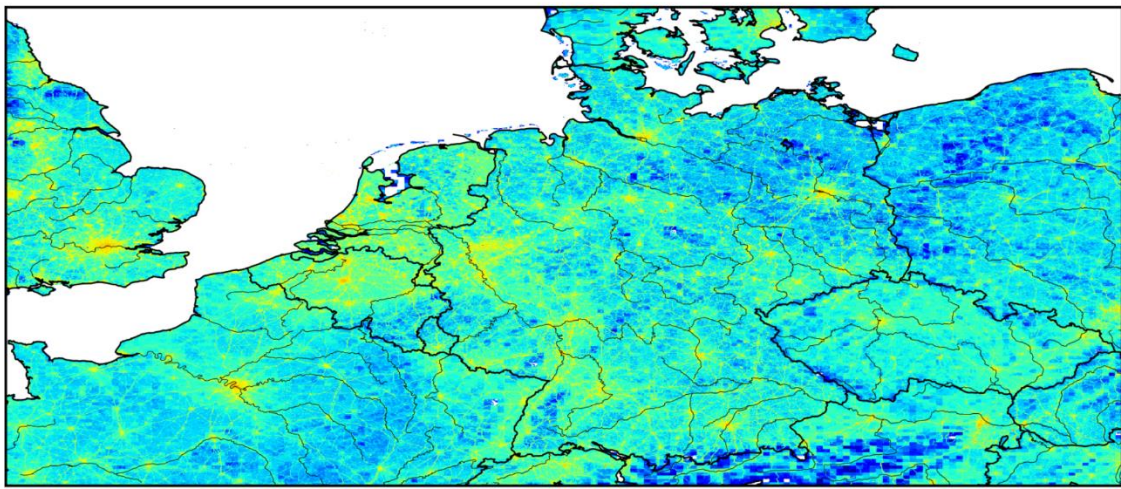
440 As mentioned before, the uncertainty of the emission value in a grid cell is determined by the uncertainties in  
441 activity data, emission factors and spatial distribution proxies. The gridded uncertainty maps in Figure 14 and  
442 Figure 15 illustrate that countries or (types of) regions differ significantly in their emission uncertainty, both in  
443 absolute and relative values. Concerning the uncertainty in CO<sub>2</sub> and CO emissions, several observations can be  
444 made.

445 First, for both CO and CO<sub>2</sub> the road network is visible due to low relative uncertainties and high absolute  
446 uncertainties compared to the surroundings. This indicates that, despite having large emissions per pixel, the  
447 spread in road traffic emissions among ensemble members is relatively small. This is likely due to the small  
448 (normally distributed) uncertainty in the spatial proxies for road traffic, i.e. the location of the roads is well-known.  
449 The surrounding rural areas are dominated by other stationary combustion, which has a slightly larger spatial  
450 uncertainty.

### Total CO<sub>2</sub>



0.05 0.10 0.15 0.20 0.25 0.30 0.35 0.40  
Relative uncertainty



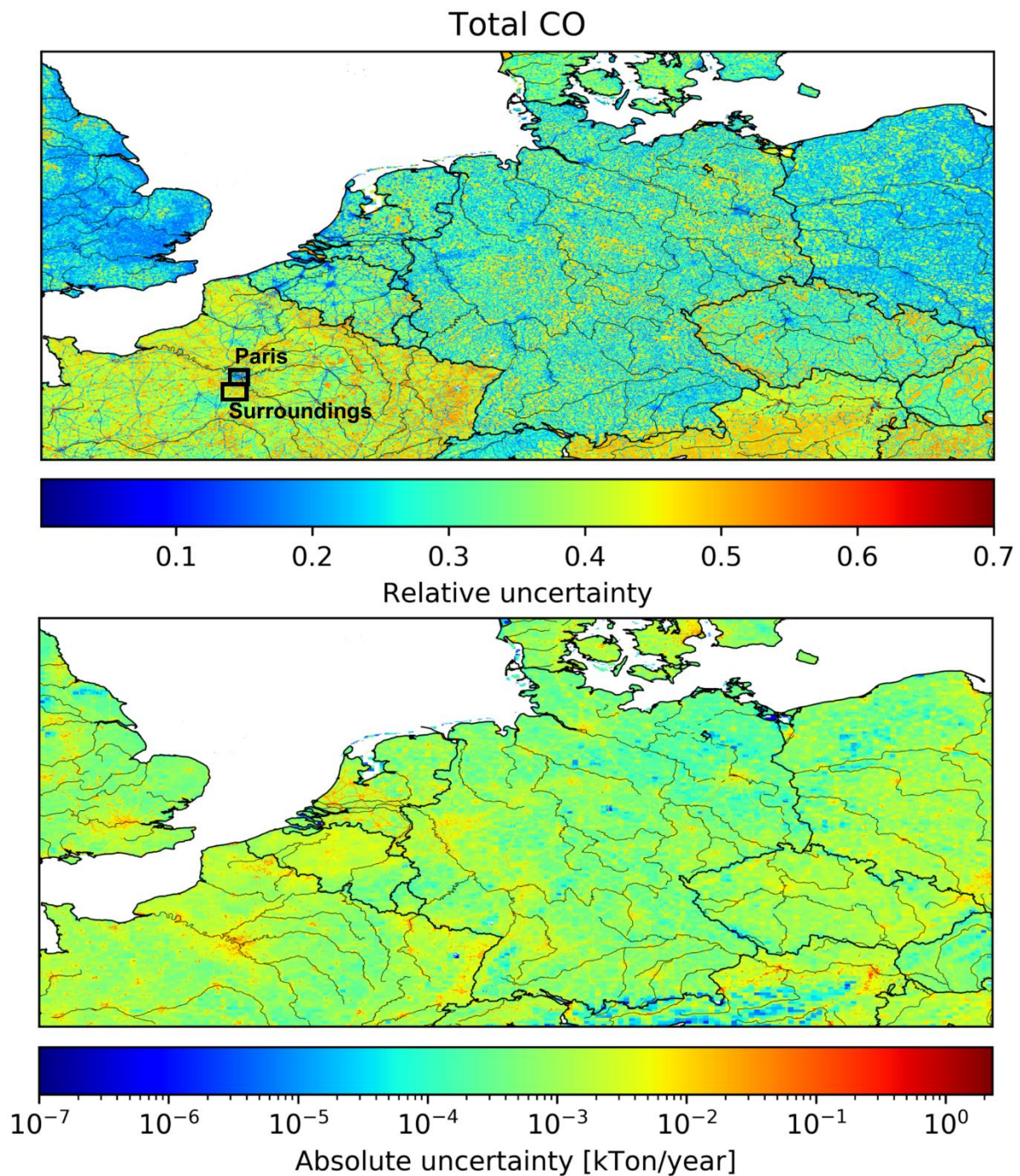
10<sup>-4</sup> 10<sup>-3</sup> 10<sup>-2</sup> 10<sup>-1</sup> 10<sup>0</sup> 10<sup>1</sup> 10<sup>2</sup> 10<sup>3</sup>  
Absolute uncertainty [kTon/year]

451

452

453

Figure 14: Maps of the relative and absolute uncertainty in CO<sub>2</sub> emissions. Areas that are examined in more detail are outlined by black squares in the top panel.

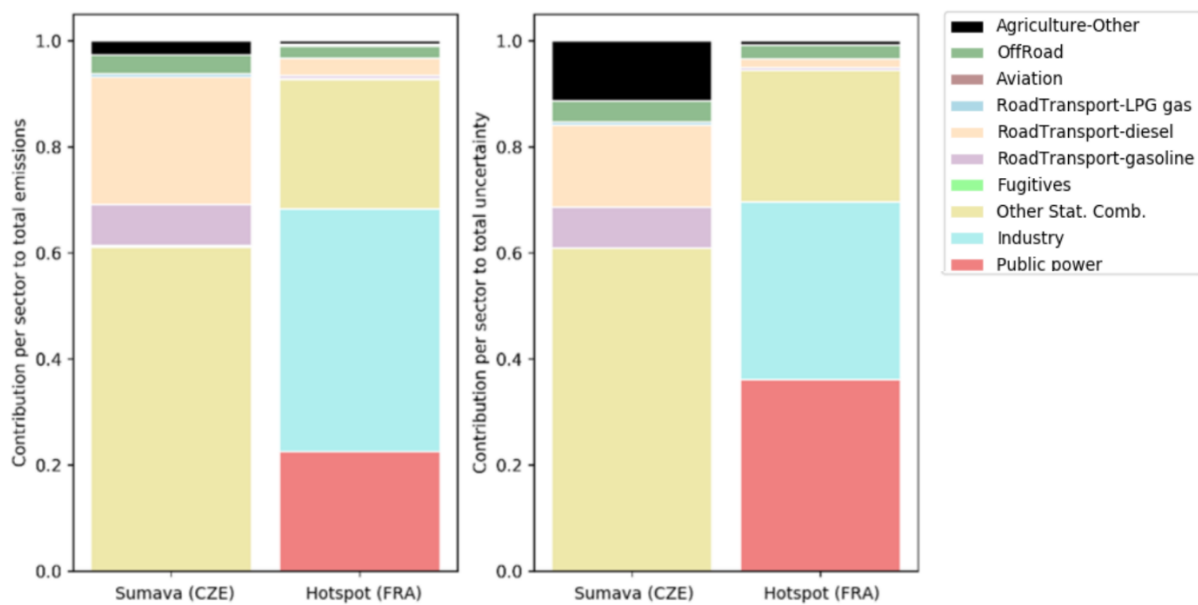


454

455 **Figure 15: Maps of the relative and absolute uncertainty in CO emissions. Areas that are examined in more detail are**  
 456 **outlined by black squares in the top panel.**

457 Second, in Austria (Tirol mainly) a large area of high relative uncertainty in CO<sub>2</sub> emissions is visible (average  
 458 pixel emission is 220 tonnes CO<sub>2</sub> yr<sup>-1</sup>), which we compare to an area just on the other side of the border in southern  
 459 Germany (average pixel emission is 495 tonnes CO<sub>2</sub> yr<sup>-1</sup>). The uncertainty in both areas is dominated by other  
 460 stationary combustion. Yet, in Austria a lot of biofuels are is used (52 % of the total emissions for this source  
 461 sector) with a large uncertainty in the emission factor and spatial distribution, whereas in Germany only 20 % of  
 462 the emissions in this sector are caused by biofuels combustion. On the other hand, the absolute uncertainty is very  
 463 small in Tirol because of the low population density (and thus small emissions) in this mountainous area.

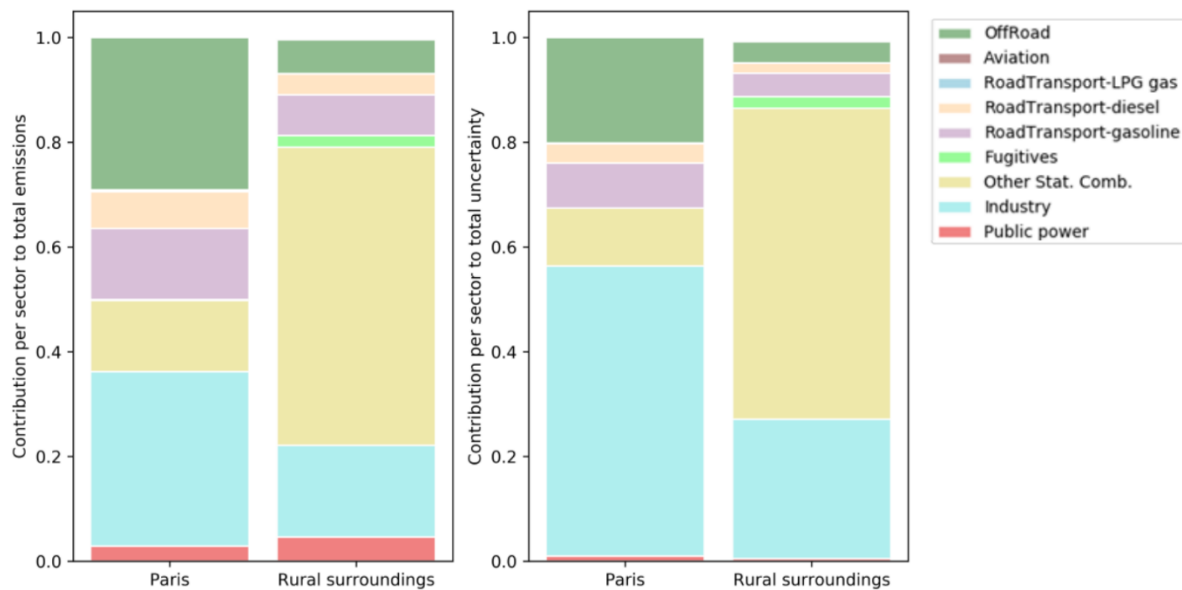
464 Third, some large patches of high relative uncertainty in CO<sub>2</sub> emissions are visible in the Czech Republic and the  
 465 northeast of France. The location of these patches seems to correspond to natural areas/parks. Therefore, absolute  
 466 uncertainties are low in these areas given the low emissions (average pixel emission in the Sumava national park  
 467 is 22 tonnes CO<sub>2</sub> yr<sup>-1</sup>). The total uncertainty can be explained for 60 % by the uncertainty in other stationary  
 468 combustion, mainly wood burning (Figure 16). Also, agriculture (field burning of residues) plays a significant  
 469 role. In addition to these natural areas, there are also some very small dark red areas (relative uncertainty) in  
 470 northern France. These areas are military domain and have a lower absolute uncertainty than their surroundings  
 471 because very few emissions are distributed to these areas (average pixel emission is 250 tonnes CO<sub>2</sub> yr<sup>-1</sup>). The  
 472 public power and industrial emissions are probably too small to be reported, hence the large relatively uncertainty.  
 473



474  
 475 **Figure 16: Contribution of source sectors to the total emissions (left) and the total uncertainty (right) in CO<sub>2</sub> for the**  
 476 **Sumava national park in the Czech Republic and a hotspot in France, summing to 100 %.** See Figure 14 for the exact  
 477 **location of these areas.**

478 Fourth, big cities/strongly urbanized areas like Paris, Berlin-the Ruhr area in Germany and Brussels-Rotterdam  
 479 (also see Fig. 1 for their locations) are clearly visible as areas where the relative uncertainty in CO emissions is  
 480 lower than in the surrounding areas. Compared to its surroundings, the uncertainty in Paris is mainly determined  
 481 by the industrial sector (Figure 17). Since industrial emissions are relatively well-known, the relative uncertainty  
 482 is small. However, the absolute uncertainty is large for big cities because of the high emissions in these densely  
 483 populated areas (average pixel emission is 64 tonnes CO yr<sup>-1</sup> for Paris). In the surrounding areas the emissions are  
 484 again dominated by other stationary combustion, which has a larger uncertainty. Yet, the absolute uncertainty is  
 485 smaller because of the lower emissions (average pixel emission is 12 tonnes CO yr<sup>-1</sup>).

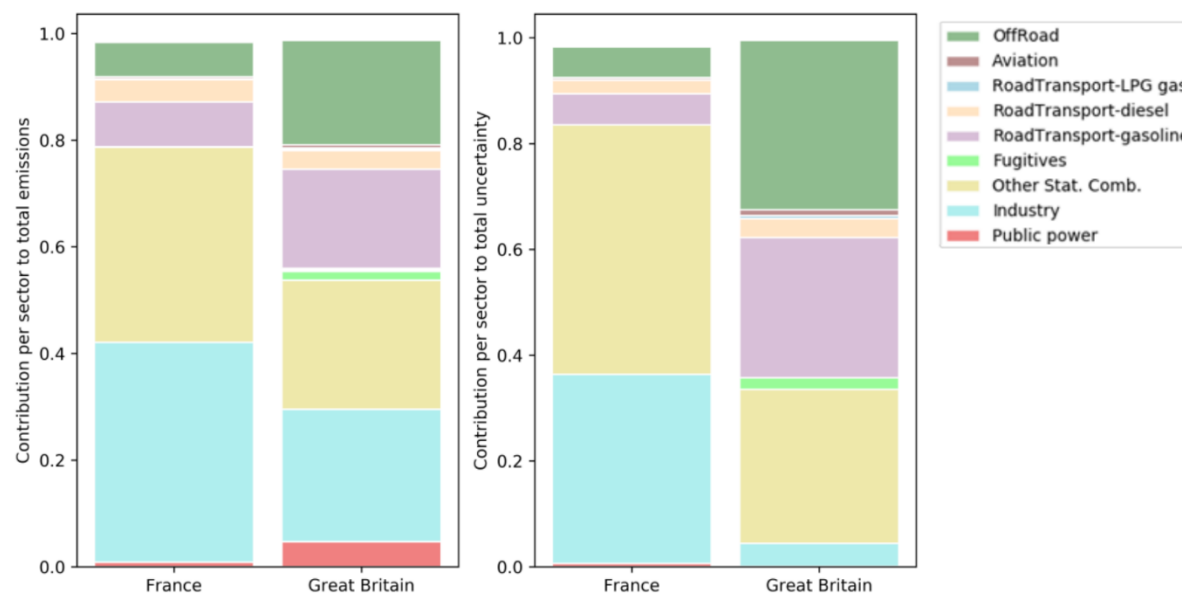




486

487 **Figure 17: Contribution of source sectors to the total emissions (left) and the total uncertainty (right) in CO for Paris**  
 488 **and its surroundings, summing to 100 %. See Figure 15 for the exact location of these areas.**

489 Finally, the relative uncertainties seem to be consistently higher in some countries than in others. For example,  
 490 the relative uncertainty in the total emissions of France and Great Britain (only pixels within the domain) are 39  
 491 % and 25 %, respectively. For France, the main sources of uncertainty are industry and other stationary  
 492 combustion, whereas the off-road and road transport sectors have a significant contribution to the uncertainty in  
 493 Great Britain (Figure 18). The main difference between the countries is again the amount of biomass used in the  
 494 other stationary combustion sector (26 % in France and 8 % in Great Britain). This is likely to explain why in  
 495 rural areas the relative uncertainty is much higher in France.



496

497 **Figure 18: Contribution of source sectors to the total emissions (left) and the total uncertainty (right) in CO for France**  
 498 **and Great Britain, summing to 100 %.**

#### 499 **4. Discussion ~~and conclusions~~**

500 Several previous studies have examined the uncertainty in emissions, either globally or nationally. For example,  
501 Andres et al. (2014) studied the uncertainty in the CDIAC emission inventory on a global scale, suggesting that  
502 the largest uncertainties are related to the fuel consumption (i.e. activity data). A similar concern was identified  
503 for China, for which the uncertainty in energy statistics resulted in an uncertainty ratio of 15.6 % in the 2012 CO<sub>2</sub>  
504 emissions (Hong et al., 2017). In the present study the uncertainties in activity data and emission factors are similar  
505 for CO<sub>2</sub>, whereas the uncertainty in CO emission factors is much larger than the uncertainty in activity data. A  
506 possible explanation for this is that the energy statistics for the European countries included here are more reliable  
507 than for developing countries. The occurrence of large differences in the reliability of reported emissions between  
508 countries is also illustrated by Andres et al. (2014). In addition to these scientific studies, many countries report  
509 uncertainties in emission estimates in their National Inventory Reports (UNFCCC, 2019). Yet, their methods for  
510 uncertainty calculation differ and can even vary over time. Several scholars have examined the uncertainty in  
511 national CO<sub>2</sub>-greenhouse gas emissions in more detail. For example, Monni et al. (2004) (Finland) and Fauster et  
512 al. (2011) (Denmark) used a Tier 2 approach (Monte Carlo simulation) to determine the uncertainty in the total  
513 greenhouse gas emissions (in CO<sub>2</sub> equivalents). They found an uncertainty of about 5–6 % for the year 2001 for  
514 Finland and an uncertainty of 4–5 % for the year 2008 for Denmark, also considering non-normal distributions in  
515 uncertainties. Moreover, Oda et al. (2019) found a 2.2 % difference in total CO<sub>2</sub> emissions in Poland between two  
516 emission inventories, which is in agreement. These values agree with our total CO<sub>2</sub> emission uncertaintyies.

517 Even fewer studies have focused on uncertainties in the proxy maps used for spatial disaggregation. Some studies  
518 compared emission inventories to get an idea of the spatial uncertainties (Gately and Hutyra, 2017; Hutchins et  
519 al., 2017), but these studies are likely to underestimate uncertainties due to systematic errors caused that occur  
520 when different emission inventories use similar methods and/or proxies for spatial allocation. Moreover, exact  
521 quantification of uncertainties is often limited, dependent on the spatial scale, and the uncertainties are not  
522 specified per source (i.e. total emissions and spatial disaggregation) (Oda et al., 2019). Sowden et al. (2008) used  
523 a qualitative approach to identify the uncertainty of different components of their emission inventory for reactive  
524 pollutants (activity, emission factors, spatial and temporal allocation and speciation) by giving each component a  
525 quality rating. They suggest that spatial allocation is an important source of uncertainty for residential burning,  
526 but not so much for point sources and road traffic. Indeed, the location of large point sources and roads is relatively  
527 well-known. However, we consider the allocation of emissions to pixels that include roads to have a significant  
528 (pixel value) uncertainty. Therefore, our results show that uncertainties in the spatial proxy used for road traffic  
529 can cause a significant spread in CO concentrations.

530 Andres et al. (2016) did a more extensive analysis of the spatial distribution in CDIAC, including uncertainties in  
531 pixel values (e.g. due to incorrect accounting methods or changes over time) and due to the representativeness of  
532 the proxy for the spatial distribution of emissions (also see Sect. 2.2.3). We considered these sources of uncertainty  
533 as well. However, Andres et al. (2016) also mention spatial discretization as a source of error, because they assign  
534 each pixel (1x1° resolution) to one country. The proxy maps used in this study include country fractions in each  
535 pixel, reducing this uncertainty. In contrast, we suggest another source of uncertainty, namely the fact that some  
536 pixels can include emissions while no activity takes place there or vice versa (proxy quality). Based on the listed  
537 uncertainties, Andres et al. (2016) found an average uncertainty (2σ) in individual pixels of 120 % (assuming  
538 normal distributions). Here, we find an average uncertainty (2σ) of 36 %. However, a small number of large

539 outliers occurs (less than 0.01 % of the pixels has an uncertainty of >1000 %) due to lognormal error distributions,  
540 although these are related to pixels with small emissions. A large part of the difference can be explained by the  
541 large pixel size of CDIAC and the large error introduced by spatial discretization (e.g. due to pixels that cover  
542 large areas of two different countries). Also, their emissions are spatially distributed based on population density,  
543 while we use a range of proxy maps depending on the source sector and use specific locations for large point  
544 sources. However, the uncertainty estimates are partially based on expert judgement and remain subjective.  
545 Moreover, the uncertainty related to the location of actual activities is not included in our uncertainty estimate,  
546 even though we have shown this can have a large impact locally.

547 The country-level CO<sub>2</sub> emissions used for our emission inventory are based on NIR's, which are assumed to be  
548 relatively accurate because of the use of detailed fuel consumption statistics and country-specific emission factors  
549 (Andres et al., 2014; Francey et al., 2013). The uncertainties reported in the NIRs were determined following  
550 specified procedures and are deemed the most complete and reliable estimates available. Yet, because of the use  
551 of prescribed methods and in some cases general emission factors, systematic errors can occur both in the estimate  
552 of parameters and in the estimate of uncertainties. We choose to average the uncertainties reported by several  
553 countries, because the uncertainty estimates are relatively consistent across countries. However, this would not  
554 eliminate such systematic errors. The effect of systematic errors could be analysed by comparing different sources  
555 of information. Additionally, we assume point source emissions are relatively certain, yet a recent study showed  
556 that significant uncertainties exist in reported emissions of US power plants (Quick and Marland, 2019). A similar  
557 study for Europe is recommended, not only to improve the knowledge for the European situation, but also to  
558 understand continental differences.

559 One source of uncertainty that is not considered in this study is the incompleteness of the emission inventory (i.e.  
560 if sources are missing) or double-counting errors. For example, during the compilation of the base inventory we  
561 found that in several cases the CO<sub>2</sub> emissions from airports were very low. The reason was that emissions from  
562 international flights are not reported in the NIR's and are therefore not part of the emission data used to create the  
563 inventory. Once discovered, this was corrected and ~~LTO~~ (aircraft landing and take-off) emissions from  
564 international flights were added in a later stage. Such discrepancies caused by reporting guidelines could be  
565 present for other source types as well. Although overall this error is likely to be small, locally the errors might be  
566 significant.

567 Finally, Sowden et al. (2008) mention (dis)aggregation as another source of error, i.e. the calculation of emissions  
568 on a different scale (spatially, temporally or sector level) than the input data. In principle, fuel consumption data  
569 is available on aggregated levels and then separated over different subsectors. This increases the uncertainty at  
570 the lower level, but on the aggregated level the uncertainties remain the same. A similar note was made by Andres  
571 et al. (2016) about the use of higher resolution proxy maps, which might increase the uncertainty due to lack of  
572 local data. However, when local data is available this might also decrease the uncertainties. For example, the  
573 EDGAR emission database uses non-country specific emission factors based on technology levels and sector  
574 aggregated energy statistics (Muntean et al., 2018). The reason is that the level of detail we used in this paper is  
575 not available globally. However, using generic emission factors can introduce large uncertainties when sub-  
576 sectoral changes occur. Therefore, regional/local studies could benefit from using a dedicated emission inventory  
577 for their region of interest instead of a global inventory.

578 Our results can be used to support network design and inverse modelling. The uncertainty maps are helpful to  
579 identify regions with large emission uncertainties, which can be the focus point of an inversion with the aim to  
580 optimize emissions in those regions. However, inverse modelling requires an observational network that is  
581 sensitive to the emissions from the regions of interest. A site is sensitive to specific emissions when it is often  
582 affected by them, taking into account the dominant wind direction and the magnitude of concentration  
583 enhancements, which should be larger than the uncertainties that affect model-observation comparison (e.g.  
584 measurement uncertainty and model errors). Plumes from emission hot spots can travel a long distance and sites  
585 up to 30 km downwind have shown to be able to detect urban signals (Super et al., 2017a; Turnbull et al., 2015).  
586 The concentration enhancement in these plumes is large and therefore easy to detect. In contrast, the concentration  
587 enhancements of a single source (sector) are much smaller, as shown in Fig. 10 and Fig. 11, and therefore they  
588 become undetectable at much shorter distances. For example, vehicle exhaust emissions were shown to decrease  
589 by a factor 2 at 200 m from a highway (Canagaratna et al., 2010), while power plants plumes have been detected  
590 several kilometres downwind (Lindenmaier et al., 2014). Dilution is strongly dependent on the atmospheric  
591 conditions and also the height of the measurement site plays an important role. To conclude, the optimal network  
592 design is strongly dependent on which question needs to be answered and the focus area and resolution needed to  
593 reach this goal.

## 594 5. Conclusions

595 In this work we studied the uncertainties in a high-resolution gridded emission inventory for CO<sub>2</sub> and CO,  
596 considering uncertainties in the underlying parameters (activity data, emission factors, spatial proxy maps and  
597 ~~time-temporal~~ profiles). We find that all factors play a significant role in determining the emission uncertainties,  
598 but that the contribution of each factor differs per sector. Disaggregation of emissions introduces additional  
599 sources of uncertainty, which makes uncertainties at higher resolution larger than at the scale of a country/year  
600 and can have a large impact on (the interpretation of) local measurements. This is an important consideration for  
601 inverse modelers and our methodology can be used to better define local uncertainties for e.g. urban inversions.  
602 Inverse modelers should be aware that the use of erroneous ~~time-temporal~~ profiles to extrapolate emission data  
603 could result in errors of a few percent, which for CO<sub>2</sub> is significant. In the future, the temporal profiles could be  
604 improved by using detailed activity data, e.g. from power plants. Moreover, we found that large regional  
605 differences exist in absolute and relative uncertainties. By looking in more detail at specific regions (or countries)  
606 more insight can be gained about the emission landscape and ~~what are~~ the main causes of uncertainty.  
607 Interestingly, areas with larger absolute uncertainties often have smaller relative uncertainties. A likely  
608 explanation is that large sources of CO<sub>2</sub> and CO emissions received more attention and are therefore relatively  
609 well-constrained, for example in the case of large point sources. Nevertheless, since we are most interested in  
610 absolute emission reductions the map with absolute uncertainties can be used to define an observational network  
611 that is able to reduce the largest absolute uncertainties. Finally, we believe that an uncertainty product based on a  
612 well-defined, well-documented and systematic methodology could be beneficial for the entire modelling  
613 community and support decision-making as well. However, specific needs can differ significantly between  
614 studies, for example the scale/resolution, source sector aggregation level, and which species are included.  
615 Therefore, the creation of a generic uncertainty product is challenging and needs further research.

616 **Data availability**

617 The family of ten emission inventories ~~are~~is available for non-commercial applications and research  
618 (<https://doi.org/10.5281/zenodo.3584549>). ~~Please contact Hugo Denier van der Gon (-).~~

## Appendix A

**Table A1: Relative uncertainties (fraction) in activity data and CO<sub>2</sub> emission factors as taken from the NIRs (country-average) and in CO emission factors as derived from literature (assumed equal for all countries in the domain). The quoted uncertainty ranges are assumed to be representative for one standard deviation. Uncertainties in activity data and CO<sub>2</sub> emission factors are often relatively low and symmetrically distributed and normal distributions (Norm) are assumed for these activities. Compared to CO<sub>2</sub> emission factors, the uncertainty in CO emission factors is much higher, up to an order of magnitude. Uncertainties in CO emission factors are often lognormally distributed (Logn) and are assumed equal for all countries in the HR domain. The uncertainty in the activity of open burning of waste (not covered by the NIRs) is also assumed to have a lognormal distribution.**

Sector (NFR)	Fuel type	Activity data		CO <sub>2</sub> emission factors		CO emission factors	
		Average	Distribution	Average	Distribution	Average	Distribution
Public electricity and heat production (1.A.1.a)	Solid (fossil)	0.018	Norm	0.030	Norm	0.149	Logn
	Liquid (fossil)	0.022	Norm	0.031	Norm	0.399	Norm
	Gaseous (fossil)	0.021	Norm	0.015	Norm	0.513	Norm
	Biomass	0.060	Norm	0.05	Norm	0.231	Logn
Oil and gas refining (1.A.1.b & 1.B.2.d)	All	0.038	Norm	0.048	Norm	0.402	Norm
Oil production & Gas exploration (1.B.2 mainly flaring, 1.B.2.c)	All	0.118	Norm	0.141	Norm	0.240	Logn
Iron and steel industry (1.A.2.a & 2.C.1)	All	0.044	Norm	0.056	Norm	0.240	Logn
Non-ferrous metals (1.A.2.b & 2.C.2_3)	All	0.031	Norm	0.029	Norm	0.208	Norm
Chemical industry (1.A.2.c & 2.B)	All	0.042	Norm	0.041	Norm	0.138	Logn
Pulp and paper industry (1.A.2.d)	All	0.027	Norm	0.016	Norm	0.138	Logn
Food processing, beverages and tobacco (1.A.2.e)	All	0.029	Norm	0.017	Norm	0.138	Logn
Non-metallic minerals (1.A.2.f & 2.A)	All	0.032	Norm	0.041	Norm	0.384	Logn
Other manufacturing industry (1.A.2.g)	All	0.029	Norm	0.014	Norm	0.138	Logn
Civil aviation - LTO (1.A.3.a)	All	0.089	Norm	0.040	Norm	0.231	Logn
Road transport (all vehicle types) (1.A.3.b)	Gasoline (fossil)	0.031	Norm	0.025	Norm	0.284	Logn
	Diesel (fossil)	0.032	Norm	0.026	Norm	0.319	Norm
	Gaseous (fossil)	0.039	Norm	0.027	Norm	0.320	Logn
	LPG	0.039	Norm	0.027	Norm	0.462	Norm
Other transport (1.A.3.e & 1.A.4 mobile)	All	0.067	Norm	0.023	Norm	0.384	Logn
Other mobile (1.A.5.b)	All	0.098	Norm	0.026	Norm	0.384	Logn
Residential (1.A.4.b)	Gaseous (fossil)	0.040	Norm	0.022	Norm	0.141	Logn
	Liquid (fossil)	0.048	Norm	0.024	Norm	0.404	Norm
	Solid (fossil)	0.085	Norm	0.041	Norm	0.141	Logn
	Biomass	0.163	Norm	0.055	Norm	0.384	Logn
Commercial institutional (1.A.4.a)	Gaseous (fossil)	0.043	Norm	0.022	Norm	0.138	Logn
	Liquid (fossil)	0.055	Norm	0.023	Norm	1.065	Norm
	Solid (fossil)	0.087	Norm	0.040	Norm	0.994	Norm
	Biomass	0.103	Norm	0.055	Norm	0.730	Logn

Agriculture/Forestry/Fishing (1.A.4.c)	Gaseous (fossil)	0.050	Norm	0.028	Norm	0.138	Logn
	Liquid (fossil)	0.051	Norm	0.029	Norm	1.065	Norm
	Solid (fossil)	0.095	Norm	0.048	Norm	0.994	Norm
	Biomass	0.096	Norm	0.09	Norm	0.730	Logn
Other stationary (1.A.5.a)	Gaseous (fossil)	0.097	Norm	0.023	Norm	0.138	Logn
	Liquid (fossil)	0.084	Norm	0.021	Norm	1.065	Norm
	Solid (fossil)	0.103	Norm	0.033	Norm	0.994	Norm
	Biomass	0.180	Norm	0.04	Norm	0.730	Logn
Agricultural waste burning (3.F)	-	1.609	Logn	0.2	Norm	0.429	Norm
Uncontrolled waste burning (5.C.2)	-	1.609	Logn	0.5	Norm	0.366	Logn

**Table A2: Relative uncertainties (fractions) at cell level resulting from the spatial distribution. The values listed represent the (one standard deviation) uncertainty of the emission per cell due to uncertainty sources 2 and 3 as listed in Sect. 2.2.3. All values in the table below are based on expert quantification and inevitably include a considerable amount of subjectivity. The data should therefore be considered as a first order indication only. Note that the natural logarithm (Ln) of the uncertainty fraction is given in case uncertainty has a lognormal distribution.**

Sector name	Proxy name	Distribution	Uncertainty
Public electricity and heat production; Chemical industry; Food processing, beverages and tobacco (comb); Food and beverages industry; Other non-metallic mineral production; Small combustion - Commercial/institutional – Mobile	CORINE_2012_Industrial_area	Logn	2.2
Solid fuel transformation; Iron and steel industry (comb); Iron and steel production; Pulp and paper industry (comb); Pulp and paper industry; Non-metallic minerals (comb); Cement production	CORINE_2012_Industrial_area	Logn	3.7
Other manufacturing industry (comb); Other industrial processes; Manufacturing industry - Off-road vehicles and other machinery	CORINE_2012_Industrial_area	Logn	1.4
Oil and gas refining (comb); Oil and gas refining	CORINE_2012_Industrial_area	Logn	3.7
	TNO_PS for Refineries	Logn	1.7
Coal mining (comb)	CORINE_2012_Industrial_area	Logn	4.6
	TNO_PS for Coal mining	Logn	1.7
Oil production (comb)	CORINE_2012_Industrial_area	Logn	1.7
	TNO_PS for Oil production	Logn	1.7
Gas exploration (comb)	CORINE_2012_Industrial_area	Logn	1.7
	TNO_PS for Gas production	Logn	1.7
Coke ovens (comb)	CORINE_2012_Industrial_area	Logn	1.7
	TNO_PS for Iron and steel - Coke ovens	Logn	1.7
Non-ferrous metals (comb); Other non-ferrous metal production	CORINE_2012_Industrial_area	Logn	3.7
	TNO_PS for Non-ferrous metals - Other	Logn	1.7
Aluminium production	CORINE_2012_Industrial_area	Logn	3.7
	TNO_PS for Non-ferrous metals - Aluminium	Logn	1.7
Chemical industry (comb)	CORINE_2012_Industrial_area	Logn	2.2
	TNO_PS for Chemical industry	Logn	1.7
Passenger cars	RoadTransport_PassengerCars	Norm	0.3
Light duty vehicles	RoadTransport_LightCommercialVehicles	Norm	0.3
Trucks (>3.5t)	RoadTransport_HeavyDutyTrucks	Norm	0.3

Buses	RoadTransport_Buses	Norm	0.3
Motorcycles	RoadTransport_Motorcycles	Norm	0.3
Mopeds	RoadTransport_Mopeds	Norm	0.5
Civil aviation – LTO	Airport distribution for year 2015	Logn	1.4
Mobile sources in agriculture/forestry/fishing	CORINE_2012_Arable_land	Logn	1.4
Other transportation, including pipeline compressors	Population_total_2015	Logn	3.7
Small combustion - Residential - Household and gardening; Other mobile combustion	Population_total_2015	Logn	1.3
Commercial/institutional	Population_total_2015	Norm	0.5
	Population_rural_2015	Logn	1.3
	Population_urban_2015	Logn	1.3
	Wood_use_2014	Logn	2.2
Residential	Population_total_2015	Norm	0.5
	Population_rural_2015	Logn	1.3
	Population_urban_2015	Logn	1.3
	Wood_use_2014	Logn	1.4
Agriculture/Forestry/Fishing	CORINE_2012_Arable_land	Logn	1.4
	Wood_use_2014	Logn	2.2
Other stationary combustion	Population_total_2015	Logn	1.3
	Population_rural_2015	Logn	1.3
	Wood_use_2014	Logn	1.4
Field burning of agricultural residues	CORINE_2012_Arable_land	Logn	2.2
	Population_total_2015	Logn	2.2
Open burning of waste	CORINE_2012_Industrial_area	Logn	3.7
	Population_rural_2015	Logn	3.7

## **Appendix B**

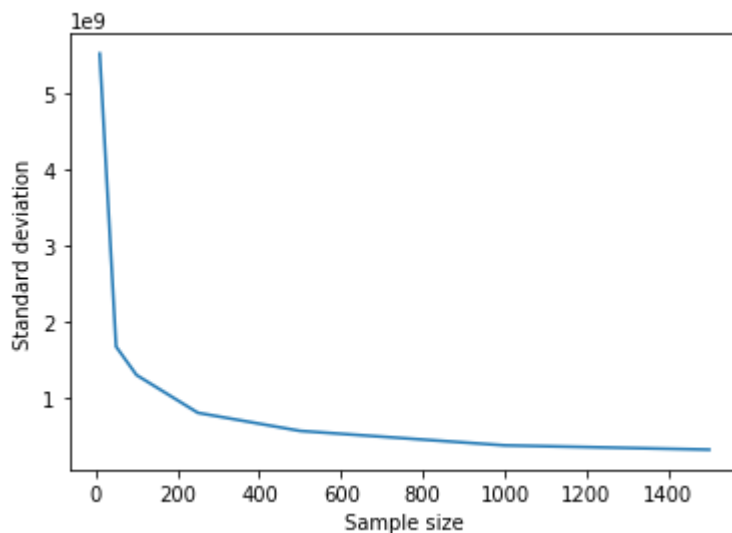


**Figure B1: Spread in the standard deviations if the Monte Carlo simulation were to be repeated multiple times for a specific sample size, based on a bootstrapping method.**



## Author contribution

A.J.H. Visschedijk assembled the uncertainty data used in this work. S.N.C. Dellaert and H.A.C. Denier van der Gon are responsible for the base emission inventory. I. Super designed the experiments, carried them out, and prepared the manuscript with contributions from all co-authors.

## Competing interests

The authors declare that they have no conflict of interest.

## Acknowledgements

This study was supported by the CO<sub>2</sub> Human Emissions (CHE) project, funded by the European Union's Horizon 2020 research and innovation programme under grant agreement No 776186 and the VERIFY project, funded by the European Union's Horizon 2020 research and innovation programme under grant agreement No 776810.

## References

- Amann, M., Bertok, I., Borcken-Kleefeld, J., Cofala, J., Heyes, C., Höglund-Isaksson, L., Klimont, Z., Nguyen, B., Posch, M., Rafaj, P., Sandler, R., Schöpp, W., Wagner, F. and Winiwarter, W.: Cost-effective control of air quality and greenhouse gases in Europe: Modeling and policy applications, *Environ. Modell. Softw.*, 26, 1489–1501, <https://doi.org/10.1016/j.envsoft.2011.07.012>, 2011.
- Andres, R. J., Boden, T. A. and Higdon, D.: A new evaluation of the uncertainty associated with CDIAC estimates of fossil fuel carbon dioxide emission, *Tellus B*, 66, <https://doi.org/10.3402/tellusb.v66.23616>, 2014.
- Andres, R. J., Boden, T. A. and Higdon, D. M.: Gridded uncertainty in fossil fuel carbon dioxide emission maps, a CDIAC example, *Atmos. Chem. Phys.*, 16, 14979–14995, <https://doi.org/10.5194/acp-16-14979-2016>, 2016.
- Berner, R. A.: The long-term carbon cycle, fossil fuels and atmospheric composition, *Nature*, 426, 323–326, <https://doi.org/10.1038/nature02131>, 2003.
- Boon, A., Broquet, G., Clifford, D. J., Chevallier, F., Butterfield, D. M., Pison, I., Ramonet, M., Paris, J. D. and Ciais, P.: Analysis of the potential of near-ground measurements of CO<sub>2</sub> and CH<sub>4</sub> in London, UK, for the monitoring of city-scale emissions using an atmospheric transport model, *Atmos. Chem. Phys.*, 16, 6735–6756, <https://doi.org/10.5194/acp-16-6735-2016>, 2016.
- Boschetti, F., Thouret, V., Maenhout, G. J., Totsche, K. U., Marshall, J. and Gerbig, C.: Multi-species inversion and IAGOS airborne data for a better constraint of continental-scale fluxes, *Atmos. Chem. Phys.*, 18, 9225–9241, <https://doi.org/10.5194/acp-18-9225-2018>, 2018.
- Breón, F. M., Broquet, G., Puygrenier, V., Chevallier, F., Xueref-Remy, I., Ramonet, M., Dieudonné, E., Lopez, M., Schmidt, M., Perrussel, O. and Ciais, P.: An attempt at estimating Paris area CO<sub>2</sub> emissions from atmospheric concentration measurements, *Atmos. Chem. Phys.*, 15, 1707–1724, <https://doi.org/10.5194/acp-15-1707-2015>, 2015.
- Canagaratna, M. R., Onasch, B. T., Wood, E. C., Herndon, S. C., Jayne, J. T., Cross, E. S., Miake-Lye, R. C., Kolb, C. E. and Worsno, D. R.: Evolution of vehicle exhaust particles in the atmosphere, *J. Air Waste Manag.*, 60, 1192–1203, <https://doi.org/10.3155/1047-3289.60.10.1192>, 2010.

Denier van der Gon, H. A. C., Hendriks, C., Kuenen, J., Segers, A. and Visschedijk, A.: Description of current temporal emission patterns and sensitivity of predicted AQ for temporal emission patterns, TNO, Utrecht, Netherlands., 2011.

Denier van der Gon, H. A. C., Kuenen, J. J. P., Janssens-Maenhout, G., Döring, U., Jonkers, S. and Visschedijk, A.: TNO\_CAMS high resolution European emission inventory 2000-2014 for anthropogenic CO<sub>2</sub> and future years following two different pathways, *Earth Syst. Sci. Data Discuss.*, 1–30, <https://doi.org/10.5194/essd-2017-124>, in review, 2017.

European Environment Agency: EMEP/EEA air pollutant emission inventory guidebook 2016: Technical guidance to prepare national emission inventories, Luxembourg., 2016.

Fausser, P., Sørensen, P. B., Nielsen, M., Winther, M., Plejdrup, M. S., Hoffmann, L., Gyldenkerne, S., Mikkelsen, H. M., Albrektsen, R., Lyck, E., Thomsen, M., Hjelgaard, K. and Nielsen, O.-K.: Monte Carlo Tier 2 uncertainty analysis of Danish Greenhouse gas emission inventory, *Greenh. Gas Meas. Manag.*, 1, 145–160, <https://doi.org/10.1080/20430779.2011.621949>, 2011.

Francey, R. J., Trudinger, C. M., Van der Schoot, M., Law, R. M., Krummel, P. B., Langenfelds, R. L., Paul Steele, L., Allison, C. E., Stavert, A. R., Andres, R. J. and Rödenbeck, C.: Atmospheric verification of anthropogenic CO<sub>2</sub> emission trends, *Nat. Clim. Change*, 3, 520–524, <https://doi.org/10.1038/nclimate1817>, 2013. Gately, C. K. and Hutyrá, L. R.: Large uncertainties in urban-scale carbon emissions, *J. Geophys. Res. Atmos.*, 122, 242–260, <https://doi.org/10.1002/2017JD027359>, 2017.

Gurney, K. R., Zhou, Y., Mendoza, D., Chandrasekaran, V., Geethakumar, S., Razlivanov, I., Song, Y. and Godbole, A.: Vulcan and Hestia: High resolution quantification of fossil fuel CO<sub>2</sub> emissions, in : MODSIM 2011 - 19th International Congress on Modelling and Simulation - Sustaining Our Future: Understanding and Living with Uncertainty, Perth, Australia., 12-16 December 2011, 1781–1787, 2011.

Gurney, K. R., Patarasuk, R., Liang, J., Song, Y., Keeffe, D., Rao, P., Whetstone, J. R., Duren, R. M., Eldering, A. and Miller, C.: The Hestia fossil fuel CO<sub>2</sub> emissions data product for the Los Angeles megacity (Hestia-LA), *Earth Syst. Sci. Data Discuss.*, 2030, 1–38, <https://doi.org/10.5194/essd-2018-162>, 2019.

Hong, C., Zhang, Q., He, K., Guan, D., Li, M., Liu, F. and Zheng, B.: Variations of China's emission estimates: Response to uncertainties in energy statistics, *Atmos. Chem. Phys.*, 17, 1227–1239, <https://doi.org/10.5194/acp-17-1227-2017>, 2017.

Hutchins, M. G., Colby, J. D., Marland, G. and Marland, E.: A comparison of five high-resolution spatially-explicit, fossil-fuel, carbon dioxide emission inventories for the United States, *Mitig. Adapt. Strat. Gl.*, 22, 947–972, <https://doi.org/10.1007/s11027-016-9709-9>, 2017.

IEA: World Energy Outlook 2008, Paris., 2008.

Van Jaarsveld, J. A.: The Operational Priority Substances model. Description and validation of OPS-Pro 4.1, RIVM, Bilthoven, Netherlands., 2004.

Janssen, H.: Monte-Carlo based uncertainty analysis: Sampling efficiency and sampling convergence, *Reliab. Eng. Syst. Safe.*, 109, 123–132, <http://doi.org/10.1016/j.res.2012.08.003>, 2013.

Kuenen, J. J. P., Visschedijk, A. J. H., Jozwicka, M. and Denier van der Gon, H. A. C.: TNO-MACC-II emission inventory; A multi-year (2003-2009) consistent high-resolution European emission inventory for air quality modelling, *Atmos. Chem. Phys.*, 14, 10963–10976, <https://doi.org/10.5194/acp-14-10963-2014>, 2014.

Lauvaux, T., Miles, N. L., Richardson, S. J., Deng, A., Stauffer, D. R., Davis, K. J., Jacobson, G., Rella, C.,

Calonder, G. P. and Decola, P. L.: Urban emissions of CO<sub>2</sub> from Davos, Switzerland: The first real-time monitoring system using an atmospheric inversion technique, *J. Appl. Meteorol. Climatol.*, 52, 2654–2668, <http://doi.org/10.1175/JAMC-D-13-038.1>, 2013.

Lindenmaier, R., Dubey, M. K., Henderson, B. G., Butterfield, Z. T., Herman, J. R., Rahn, T. and Lee, S.-H.: Multiscale observations of CO<sub>2</sub>, 13CO<sub>2</sub>, and pollutants at Four Corners for emission verification and attribution, *Proc. Natl. Acad. Sci.*, 111, 8386–8391, <http://doi.org/10.1073/pnas.1321883111>, 2014.

Monni, S., Syri, S. and Savolainen, I.: Uncertainties in the Finnish greenhouse gas emission inventory, *Environ. Sci. Policy*, 7, 87–98, <https://doi.org/10.1016/j.envsci.2004.01.002>, 2004.

Muntean, M., Vignati, E., Crippa, M., Solazzo, E., Schaaf, E., Guizzardi, D. and Olivier, J. G. J.: Fossil CO<sub>2</sub> emissions of all world countries - 2018 report, European Commission, Luxembourg., 2018.

Oda, T., Bun, R., Kinakh, V., Topylko, P., Halushchak, M., Marland, G., Lauvaux, T., Jonas, M., Maksyutov, S., Nahorski, Z., Lesiv, M., Danylo, O. and Joanna, H.-P.: Errors and uncertainties in a gridded carbon dioxide emissions inventory, *Mitig. Adapt. Strateg. Glob. Change*, 24, 1007–1050, <https://doi.org/10.1007/s11027-019-09877-2>, 2019.

Palmer, P. I., O’Doherty, S., Allen, G., Bower, K., Bösch, H., Chipperfield, M. P., Connors, S., Dhomse, S., Feng, L., Finch, D. P., Gallagher, M. W., Gloor, E., Gonzi, S., Harris, N. R. P., Helfter, C., Humpage, N., Kerridge, B., Knappett, D., Jones, R. L., Le Breton, M., Lunt, M. F., Manning, A. J., Matthiesen, S., Muller, J. B. A., Mullinger, N., Nemitz, E., O’Shea, S., Parker, R. J., Percival, C. J., Pitt, J., Riddick, S. N., Rigby, M., Sembhi, H., Siddans, R., Skelton, R. L., Smith, P., Sonderfeld, H., Stanley, K., Stavert, A. R., Wenger, A., White, E., Wilson, C. and Young, D.: A measurement-based verification framework for UK greenhouse gas emissions: an overview of the Greenhouse gAs Uk and Global Emissions (GAUGE) project, *Atmos. Chem. Phys.*, 18, 11753–11777, <https://doi.org/10.5194/acp-18-11753-2018>, 2018.

Quick, J. C. and Marland, E.: Systematic error and uncertain carbon dioxide emissions from USA power plants, *J. Air Waste Manag.*, 69, 646–658, <https://doi.org/10.1080/10962247.2019.1578702>, 2019.

Sauter, F., Van Zanten, M., Van der Swaluw, E., Aben, J., De Leeuw, F. and Van Jaarsveld, H.: The OPS-model. Description of OPS 4.5.0, RIVM, Bilthoven., 2016.

Sowden, M., Cairncross, E., Wilson, G., Zunckel, M., Kirillova, E., Reddy, V. and Hietkamp, S.: Developing a spatially and temporally resolved emission inventory for photochemical modeling in the City of Cape Town and assessing its uncertainty, *Atmos. Environ.*, 42, 7155–7164, <https://doi.org/10.1016/j.atmosenv.2008.05.048>, 2008.

Super, I., Denier van der Gon, H. A. C., Van der Molen, M. K., Sterk, H. A. M., Hensen, A. and Peters, W.: A multi-model approach to monitor emissions of CO<sub>2</sub> and CO from an urban-industrial complex, *Atmos. Chem. Phys.*, 17, 13297–13316, <https://doi.org/10.5194/acp-17-13297-2017>, 2017a.

Super, I., Denier van der Gon, H. A. C., Visschedijk, A. J. H., Moerman, M. M., Chen, H., van der Molen, M. K. and Peters, W.: Interpreting continuous in-situ observations of carbon dioxide and carbon monoxide in the urban port area of Rotterdam, *Atmos. Pollut. Res.*, 8, 174–187, <https://doi.org/10.1016/j.apr.2016.08.008>, 2017b.

Turnbull, J. C., Sweeney, C., Karion, A., Newberger, T., Lehman, S. J., Tans, P. P., Davis, K. J., Lauvaux, T., Miles, N. L., Richardson, S. J., Cambaliza, M. O., Shepson, P. B., Gurney, K., Patarasuk, R. and Razlivanov, I.: Toward quantification and source sector identification of fossil fuel CO<sub>2</sub> emissions from an urban area: Results from the INFLUX experiment, *J. Geophys. Res. Atmos.*, 120, 292–312, <http://doi.org/10.1002/2013JD020225>, 2015.

UNFCCC: National Inventory Submissions 2019, [online] Available from: <https://unfccc.int/process-and-meetings/transparency-and-reporting/reporting-and-review-under-the-convention/greenhouse-gas-inventories-annex-i-parties/national-inventory-submissions-2019>, 2019.

Zheng, B., Chevallier, F., Yin, Y., Ciais, P., Fortems-cheiney, A., Deeter, M. N., Parker, R. J., Wang, Y., Worden, H. M. and Zhao, Y.: Global atmospheric carbon monoxide budget 2000–2017 inferred from multi-species atmospheric inversions, *Earth Syst. Sci. Data Discuss.*, 1, 1–42, <https://doi.org/10.5194/essd-2019-61>, 2019.